EML 4905 Senior Design Project

A B.S. THESIS
PREPARED IN PARTIAL FULFILLMENT OF THE
REQUIREMENT FOR THE DEGREE OF
BACHELOR OF SCIENCE
IN
MECHANICAL ENGINEERING

Highway Wind Energy

Bruce Champagnie
Geatjens Altenor
Antonia Simonis

Advisor: Dr.Boesl

November 21, 2013

This B.S. thesis is written in partial fulfillment of the requirements in EML 4905. The contents represent the opinion of the authors and not the Department of Mechanical and Materials Engineering.

Ethics Statement and Signatures

The work submitted in this B.S. thesis is solely prepared by a team consisting of BRUCE CHAMPAGNIE, GEATJENS ALTENOR, and ANTONIA SIMONIS and it is original. Excerpts from others' work have been clearly identified, their work acknowledged within the text and listed in the list of references. All of the engineering drawings, computer programs, formulations, design work, prototype development and testing reported in this document are also original and prepared by the same team of students.

Antonia Simonis	Bruce Champagnie	GeatjensAltenor
Team Leader	Team Member	Team Member

Dr. Boesl

Faculty Advisor

TABLE OF CONTENTS

LIST OF FIGURES

INTRODUCTION

Wind energy is the fastest growing source of clean energy worldwide. This is partly due to the increase in price of fossil fuels and government incentives. The employment of wind energy is expected to increase dramatically over the next few years according to data from the Global Wind Energy Council. A major issue with the technology is fluctuation in the source of wind. There is a near constant source of wind power on the highways due to rapidly moving vehicles. The motivation for this project is to contribute to the global trend towards clean energy in a feasible way.

GLOBAL APPLICATIONS

Before taking on this project, we wanted to know if there was a global interest in such technology and if other countries could benefit from the research. Our wind turbine design can be used in any city around the world. It is environmentally friendly. Labels in various languages and manuals will be provided for each specific city. Figure 1 shows a dramatic increase in the employment of wind energy globally. Wind power increased by nearly 20% in 2012 reaching a new peak of 282 GW. Various sources such as the Global Wind Energy Council show China as the leading country in the employment of Wind energy.

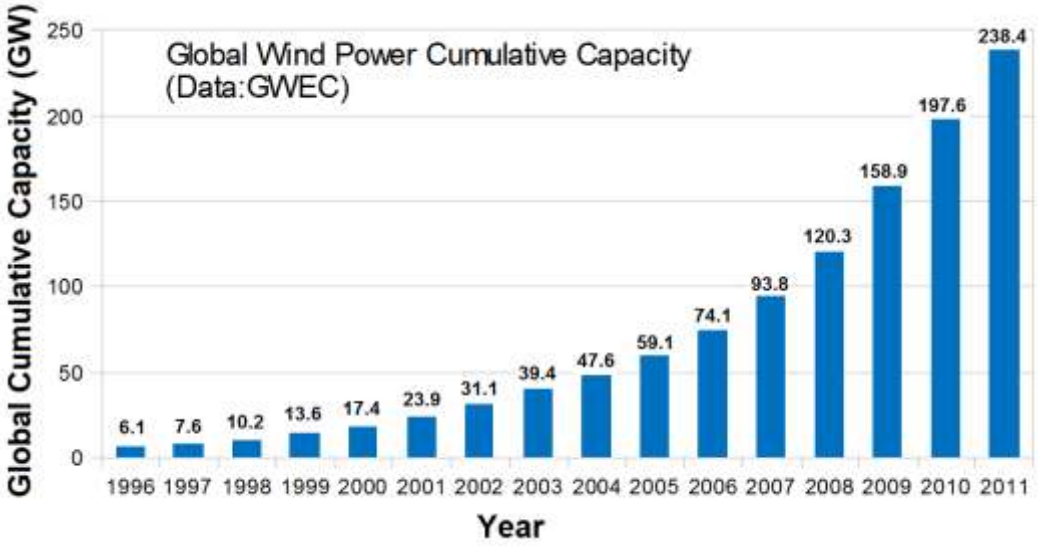

FIGURE 1. GLOBAL TREND IN WIND ENERGY GENERATION RETRIEVED FROM THE GWEC.

Nationally, wind power is on the rise due to factors such as government incentives and increasing environmental awareness. Figure 1 shows the rise in wind energy production worldwide.

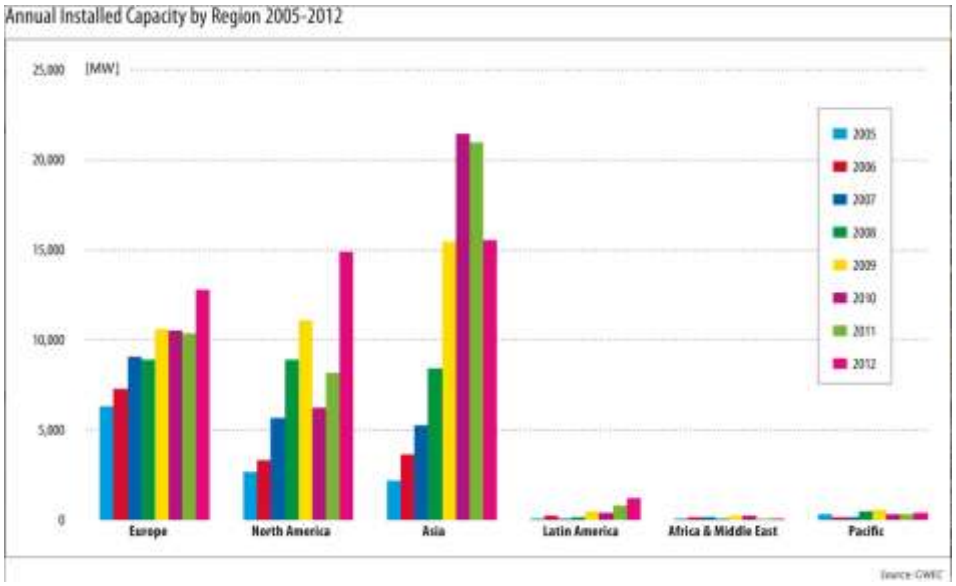

FIGURE 2. WIND TURBINE INSTALLATIONS BY REGION.

Figure 2 shows the amount of wind turbines installed by region. According to the data, Asia is leading the world in terms of wind energy production followed by North America and Europe.

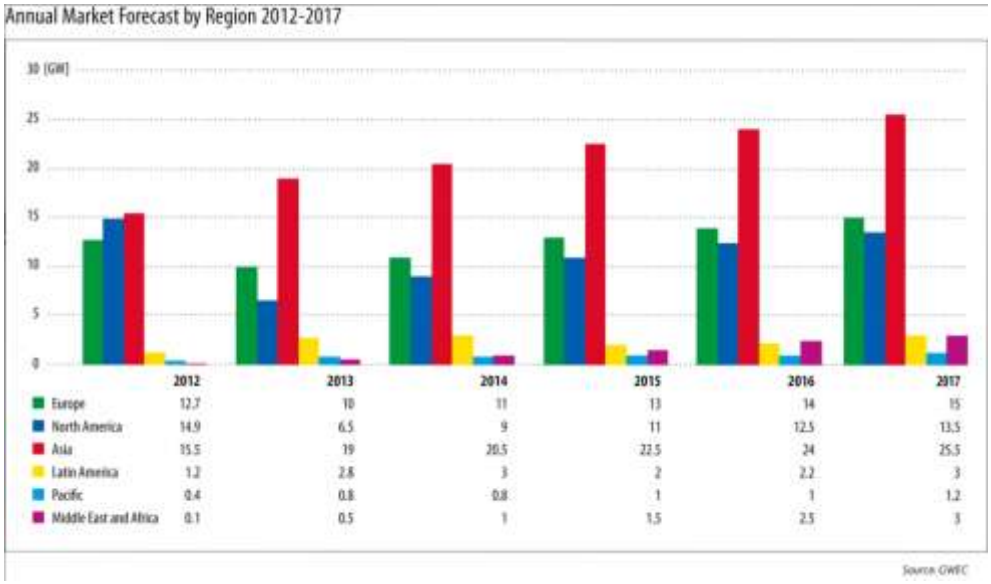

FIGURE 3. MARKET FORECAST FOR WIND TURBINES BY REGION.

Figure 3 shows the market forecast for the employment of wind energy by Region. What should be noted is that the utilization of wind energy is expected to increase in all regions over the next few years.

ABSTRACT

The objective of the project is to design a wind turbine to recapture wind energy from vehicles on the highway. Wind energy is considered the fastest growing clean energy source however; it is limited by variable natural wind. Highways can provide a considerable amount of wind to drive a turbine due to high vehicle traffic. This kinetic energy is unused. Research on wind patterns was used to determine the average velocity of the wind created by oncoming vehicles. The wind turbines are designed to be placed on the medians therefore fluid flow from both sides of the highway will be considered in the design. Using all of the collected data, existing streetlights on the medians can be fitted with these wind turbines. The design of the turbines consist of blades, collars, bearings, a shaft, gears and a generator. Additionally, since the wind source will fluctuate, a storage system for the power generated was designed to distribute and maintain a constant source of power. Ideally, the turbine can be used globally as an unlimited power source for streetlights and other public amenities.

PROBLEM STATEMENT

A major hindrance in the growth of wind energy is fluctuation in the sources of wind. Highways appear to be a sufficient source of potential wind energy. An in-depth analysis of fluid flow due to traffic on highways must be performed to acquire boundary limits for the wind turbine design. The turbine must be able to store energy for use when there is low traffic, bumper to bumper or stop and go traffic. The design must be sustainable and environmentally friendly.

MOTIVATION AND OBJECTIVE

The motivation for designing a highway wind turbine is to contribute towards the global trend in wind energy production in a feasible way. Wind turbines are traditionally employed in rural areas; the goal of this project is to design a wind turbine that can be used in cities. In particular, the turbines will use the wind draft created by vehicles on the highway to generate electricity. The idea is to offset the amount of pollution created by burning fossil fuels by introducing a potential source of clean energy.

PROJECT TIMELINE

The project is divided into several major tasks. Research is a significant portion of this project because collecting our own data requires special permissions and maybe a bit hazardous. Data is collected from the Department of Transportation and the Civil Engineering Department at FIU. All of the team members were expected to research the pros and cons of the different design options to ensure the most efficient design. The preliminary Solidworks design of the highway wind turbine was updated with new information.

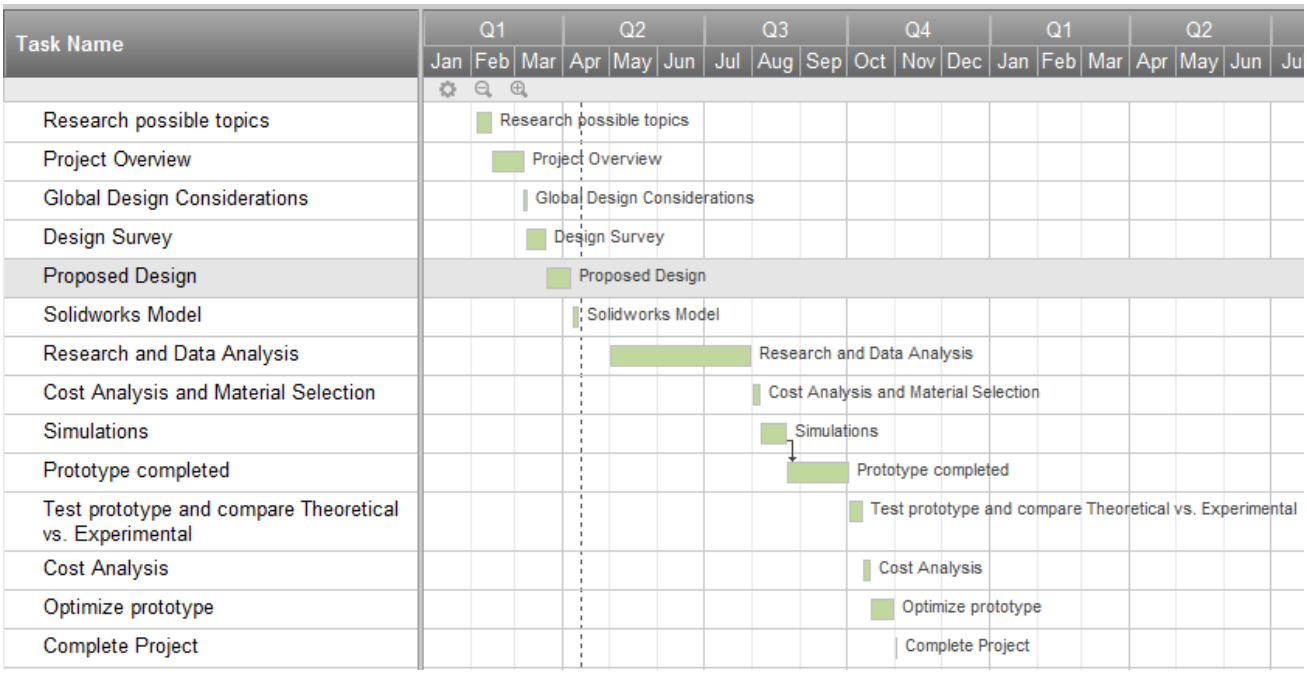

FIGURE 4: PROJECT TIMELINE

Task	Member (s)	Hours
Project Overview	All members	6
Proposed Design	Bruce Champagnie and Antonia Simonis	11
Design Survey	Bruce Champagnie	5
Preliminary Sketches	Bruce Champagnie	2
Solidworks Design	GeatjensAltenor	5
Research and Data Analysis	All members	90
Cost Analysis	GeatjensAltenor	5
Material Selection	Bruce Champagnie	5
SolidworksSimulations	Antonia Simonis	20
Design Prototype	All members	60
Testing Prototype	All members	20
Optimize Prototype	All members	48

FIGURE 5. BREAKDOWN OF TASKS

All team members are expected to participate in the research and design of the highway wind turbine. Team meetings are frequently held at least once a week. Bruce Champagnie has the most influence in collecting and analyzing relevant data relating to the turbine design. GeatjensAltenor is charged primarily with the Solidworks rendering of the turbine. Antonia Simonis is in charge of simulating and testing the completed model on Solidworks before production of the prototype. Much of the work is performed as a team but these are the areas where each individual made the most impact.

DESIGN CHALLENGES

From preliminary research it was clear that there would several challenges in completing the highway wind turbine design including costs considerations, variable wind placement and safety.

The price of wind turbines is increasing in accordance with the rising cost of energy and commodities. The cost of designing the turbine, calculated in energy savings, must be recovered in a reasonable time period.

Each vehicle on the highway offers an intermittent and uncontrolled source of wind power. The design of the wind includes storage of power and a system to distribute the generated power effectively.

Operational noise level and space are other important design considerations. The wind turbines have little negative impact on the placement location.

Wind turbines are traditionally used in remote locations. This offers the additional challenge of having to transport the power generated to the location wherein it will be utilized. Fortunately, the wind turbine in this project is designed for use in high traffic areas where the demand for power is high.

Safety was another major design consideration. The turbines must be placed in high traffic areas therefore, several safety provisions are incorporated into the design. These safety measures include stationary highway guards surrounding the rotating turbine blades and warning labels.

LITERATURE SURVEY

The idea to utilize wind turbines on the highway is not entirely unique. There have been attempts by several individuals and groups to recycle energy from highways. The most impressive is a design displayed on a YouTube video entitled "Highway Helical Wind Turbine Project (Next Generation Highway's Potential For Wind Power)." In the video a group of Mechanical Engineering Students from YCET Kollam, Kerala display a prototype of their highway wind turbine as seen in Figures 4 and 5.

FIGURE 6. COMPUTER SIMULATION OF HIGHWAY WIND TURBINE, INDIA

Figure 4 is a video still of a computer animated design of a highway wind turbine proposed by Mechanical Engineering Students in India. In Figure 5, the students Nabeel B, Firoz khan T S, Krishnaraj V, Kannan Raj, ArunS, Shaijumon T K, andAkhil Ganesh demonstrate a working prototype of their design. (Highway Helical Wind Turbine Project (Next Generation Highway's Potential For, 2012)

FIGURE 7. MECHANICAL ENGINEERING STUDENTS IN INDIA DISPLAY HIGHWAY WIND TURBINE

CONCEPTUAL DESIGN (DESIGN ALTERNATIVES)

There are several ways to approach this particular design problem. In literature surveys, we discovered different features of wind turbines that are appealing for different reasons. For example, the gear like turbines in China were very inexpensive and the modular sections could easily be snapped together to form a bigger system. That particular design did not seem as environmentally friendly as the designs with larger propellers. Other designs include turbines built into highway dividers or on overhead poles as seen in the design by the Arizona State architecture student Joe (last name not provided) (Joe, 2007). Joe calculated that with cars moving at 70 mph, 9,600 kilowatts of electricity could be produced per year using his design.

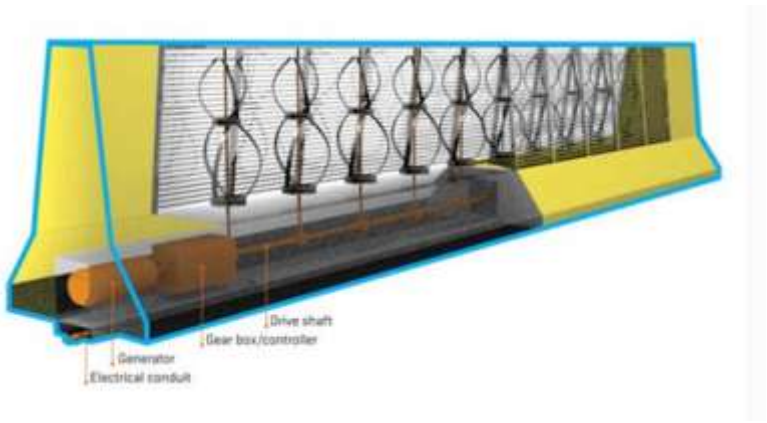

FIGURE 8. MARK OBERHOLZER, GUARDRAIL WIND TURBINE DESIGN

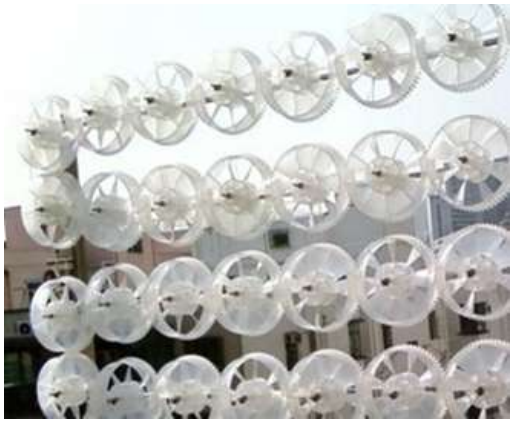

FIGURE 9. HONG KONG UNIVERSITY AND LUCIEN GAMBAROTA OF MOTORWAVE LTD.

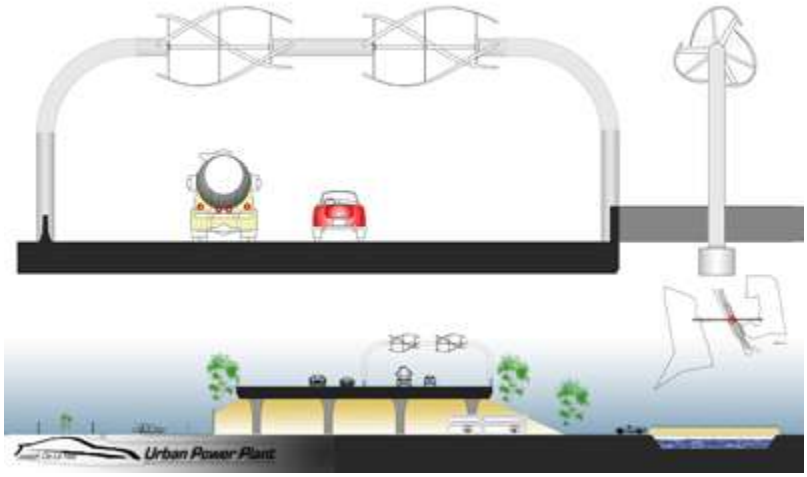

FIGURE 10. ARIZONA STATE UNIVERSITY STUDENT DESIGN

FIGURE 11. ARIZONA STATE UNIVERSITY STUDENT REALISTIC DESIGN

Figures 8-11 show various designs for wind turbines on the highway. Each design has positive and negative aspects. For example, in fig. 8, the turbines are built into guardrails. This design is particularly complex because the guardrails must be fitted with vanes in order for the wind produced by vehicles to reach the turbines inside. Figure 9 shows an inexpensive wind turbine design. This design was not selected due to safety considerations. The parts are small and can easily be snapped out of place. Figures 10 and 11 show wind turbines proposed by an Arizona State University student. This design is rejected because it may be difficult to maintain.

PROPOSED DESIGN

HOW IS WIND ENERGY CAPTURED

The movement of the wind initiated by cars implies kinetic energy. The blades of a wind turbine are constructed to capture this energy. The turbine blades rotate a shaft connected to a gearbox and generator. The mechanical energy is converted to electrical energy by the generator and may be amplified by a transformer.

WIND TURBINE SELECTION

Most people may be familiar with the horizontal axis wind turbines that dominate wind farms. These turbines have much of the major components at the top of the tower. The blades must be configured in the direction of the wind. They also have gearboxes which amplify the angular velocity of the rotating blades. The blades must be very rigid and offset a certain distance to avoid collision with the tower. Three-blade designs are generally used for commercial production of power with the assistance of computers to orient the blades into the wind.

Another major turbine configuration is the vertical axis wind turbine. There are several advantages and disadvantages to using a vertical wind turbine design. A vertical wind turbine design is selected because rotation generally commences at lower speeds. Vertical turbines are capable of capturing wind in any direction, whereas, horizontal turbines need to be pointed in the direction of the wind. The VAWT's can be operated at lower elevations. Additionally, heavy parts such as the generator and battery can easily be placed at the base of the turbine. This also makes it easier to maintain. Also, VAWTs generally have a lower noise level than HAWTs. Disadvantages include higher torque produced on the central column, lower general efficiency dynamic loading on the blades.

The two main types of VAWT's are the Darrieus and Savonius models.

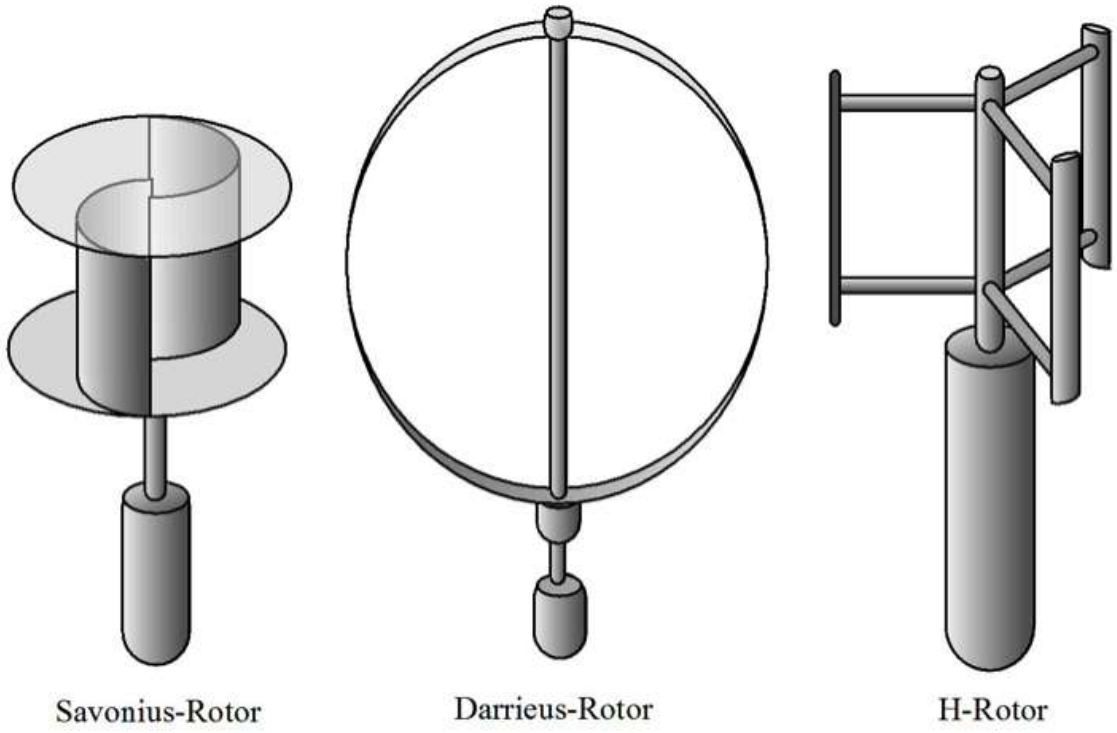

FIGURE 12. MAJOR TYPES OF WIND TURBINES

The dominant force of a Darrieus turbine is the lift force. In a Darrieus configuration, airfoil cross-sectioned blades are rotated around a central column or shaft. Georges Jean Marie Darrieus patented this design in 1931. The Darrieus model can spin many times the speed of wind. The blades have a lower solidity and are more efficient than turbines relying on the drag force however, they are not self-starting.

Savonius models have high solidity but lower efficiency. This type of VAWT was invented by Sigurd Johannes Savonius in 1922. The dominant force behind the Savonius model is the drag force. Savonius turbines have 2 or three "scoops" in an "S"configuration. The curvature of the scoops reduces the drag when moving against the wind and with the wind. Savonius configurations are often employed when cost and reliability more important than efficiency.

To make the most efficient highway wind turbine, we will be using a combination of the Darrieus and Savonius models. The Darrieus will provide better efficiency and the Savonius will aid in starting up.

MAJOR COMPONENTS

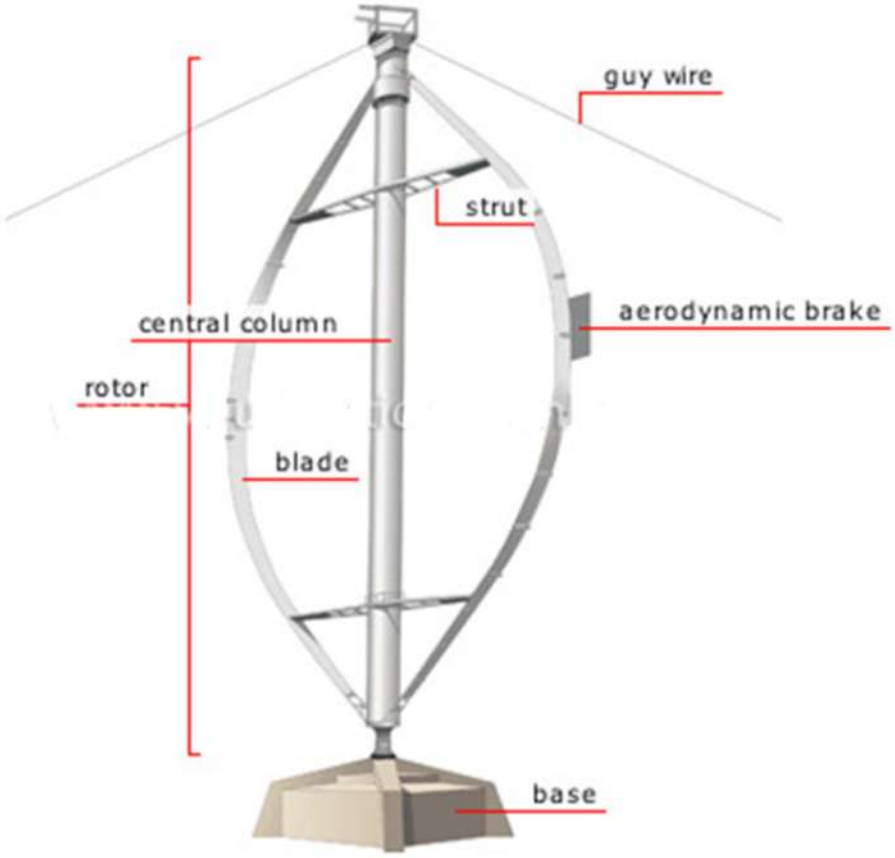

FIGURE 13. MAJOR COMPONENTS OF A VAWT

Figure 13 shows the major components of a vertical wind turbine. The most significant components are the blades, shaft and generator. The blades directly interact with the wind to transfer the kinetic energy of the moving fluid into rotational energy of the rotor. The rotor is connected to the shaft which may be connected to a gearbox or generator.

Our group designed a vertical axis wind turbine to utilize the wind produced by moving vehicles to generate electricity. These turbines will be placed along roadways that have high volume of fast moving traffic. The electricity generated will then be the stored in batteries. Since the electricity produced will be direct current (DC) it must be converted to alternating current (AC) before it can be used for lighting the street lamps, sold to the grid or any of the man ways we use electricity today. This means that the DC current must be passed through an inverter first before it is used.

The blades were the most difficult part of the design because they had to be propelled by wind in any direction. The original design called for curved blades angled so that as much surface area is exposed to the wind draft from oncoming vehicles as possible. The blades necessarily had to be lightweight. Wind turbine blades are basically modeled as airfoils. The driving forces on the blades are the lift and drag forces created by the wind. There is a difference in velocity of wind traveling on the windward and leeward side of the blade causing a difference in pressure. The Bernoulli equation can be utilized to calculate lift and drag forces when the velocity of the fluid moving on the leeward and windward side of the airfoil is known.

The central column design was relatively simple. It is a hollow tube whereon the blades are attached. It had to be strong enough to withstand the torque produced by the rotating elements.

The generator converts the mechanical energy to electrical energy through electromagnetic induction. The generator primarily consists of copper coils and magnets.

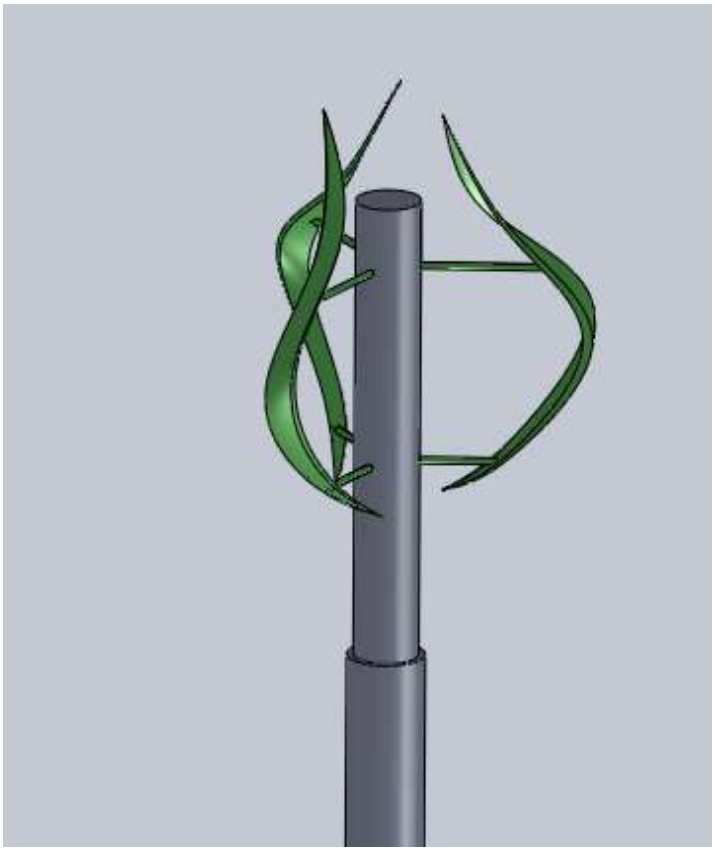

FIGURE 14. PRELIMINARY SOLIDWORKS DESIGN.

Figure 15 shows the preliminary Solidworks rendering by Geatjens Altenor. The idea was to curve and angle the blades to capture the maximum amount of wind.

To produce this product we hoped to find existing parts that fit within the design criteria and manufacture parts significant to the design. We also did a series of calculations in order to determine if the wind needed to rotate the turbines is sufficient enough to generate an adequate amount of electricity. Data was collected to determine the traffic patterns and energy storage requirements. Efficient placement is also important so that operators can harvest maximum energy from the wind draft created by automobiles.

ANALYTICAL ANALYSIS

The maximum amount of power that can be extracted from the wind is directly proportional to the air density, ρ, area swept by the turbine blades, A_s and the wind velocity, v, cubed as shown in Eq. 1 . (Hodge, 2009) This demonstrates that the most important variable in wind energy creation is the wind speed. Wind speed depends purely on the placement location and cannot be optimized therefore; the next major variable that can be optimized is the area. On the highway, wind speed can vary from 3 to as much as 8 mph roughly 5 meters from moving vehicles. For the purposes of demonstrative analysis, we will assume an average wind speed of 5 mph.

$$P_w = \frac{1}{2} \rho A_s v^3 \tag{1}$$

At standard temperature and pressure STP = 293K and 101.3 KPa, the density of air (ρ) is 1.204 kg/m^3, Eq. 1 reduces to Eq.2.

$$P_w = .602 A_s v^3 \tag{2}$$

On the highway, wind speed can vary from 3 to as much as 8 mph roughly 5 meters from moving vehicles. For the purposes of demonstrative analysis, we will assume an average wind speed of 5 mph or 2.2352 meters per second.

The area in Eq. 1 and 2 is the swept area of the turbine which depends on the diameter and blade length of the turbine as shown in Eq. 3. The area swept by the turbine is limited by the width of the median. We wanted to use a minimum amount of space to allow for the safety of pedestrians and vehicles. We limited the diameter of the turbine to 3 feet and used a blade length of 2 feet.

$$A = D_t lb \tag{3}$$

The area swept by our wind turbine is 864 in^2 or .557 m^2.

Equation 1 is the power that can be harnessed by an ideal turbine. VAWT are at best about half as efficient therefore, the actual power generated is the wind power multiplied by a coefficient of performance Cp.

$$P_m = C_p P_w \tag{4}$$

The maximum value for the power coefficient is called the Betz limit. There are losses in wind turbine efficiency due to pressure changes, drag and other factors such as power losses in the electrical system. The theoretical limit to wind turbine efficiency is 59% as given by equation 5.

$$Cp_{\max} = \frac{\frac{8}{27}\rho A V^3}{\frac{1}{2\rho C^3}} = \frac{16}{27} = 0.5926 \tag{5}$$

Wind System	Efficiency, %	
	simple Construction	Optimum Design
Multibladed farm water pump	10	30
Sailwing water pump	10	25
Darrieus water pump	15	30
Savonius windcharger	10	20
Small prop-type windcharger (up to 2kW)	20	30
Medium prop-type windcharger (2 to 10 kW)	20	30
Large prop-type wind generator (over 10 kW)	---	30 to 45
Darrieus wind generator	15	35

FIGURE 15. CP VALUES FOR VARIOUS WIND TURBINES

Figure 15 shows the typical coefficient of performance for various wind turbines.

Equation 6 is the final equation necessary to calculate the maximum power that can be extracted from the vertical wind turbine.

$$Power\ extracted = .602 C_p A_s v^3 \tag{6}$$

We used a very conservative coefficient of .30 for the hybrid Darrieus, Savonius turbine. The power we hope to extract is 1.12 joules or watt seconds. This shows the significance of gears and a power storage system.

Some analysis of fluid flow was also instrumental to the completion of the project. A Reynolds number is often employed to characterize fluid flow. In analysis of different possible turbine designs Eq. (7) defines Reynolds number.

$$Re = \frac{\rho V l}{\mu} = \frac{V l}{\nu} \tag{7}$$

In Eq.(7), V is velocity of fluid, l is a characteristic length, ρ is the density of fluid, μ is the dynamic viscosity of fluid and ν is the kinematic viscosity of the fluid. Traditionally, the characteristic length is the blade length. The calculated Reynolds number for our wind turbine is about 110000. A Reynolds number above 2000 signifies turbulent flow.

BLADES

The Darrieus turbine blades were selected first. These blades have a cross section in the shape of an airfoil such as that in Fig. 16.

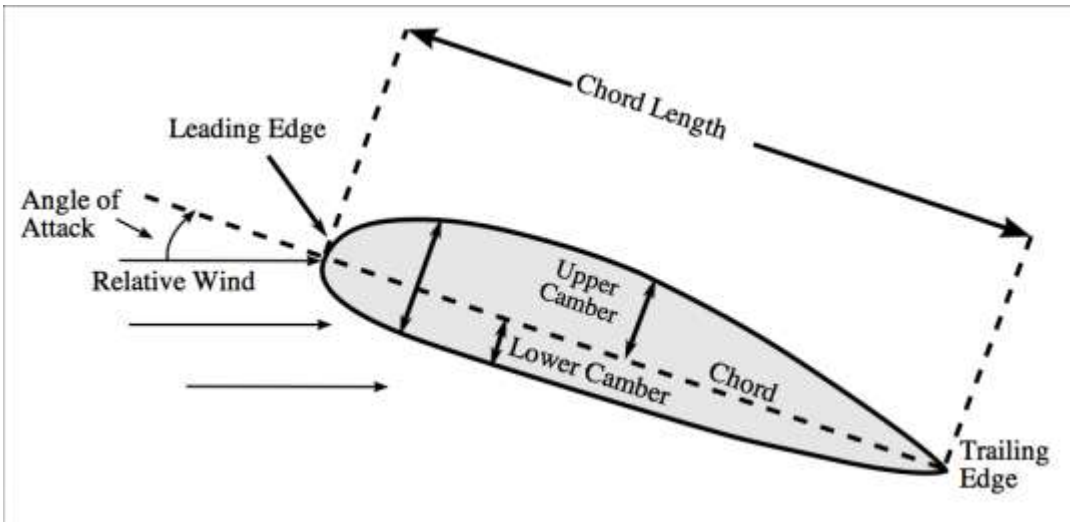

FIGURE 16. LABELLED PARTS OF AN AIRFOIL

Major features of an airfoil are labeled in Fig. 16. The leading edge is the point at the front of the airfoil with the maximum curvature. The trailing edge is the point at the extreme end of the airfoil. The chord line connects these two points. The angle of attack is the angle between the chord line and the relative direction of wind. The camber line (not pictured in Fig. 16) is median curve between the upper and lower camber. In describing an airfoil, it is important to note its maximum thickness in terms of a percentage of the chord line and the location of its maximum thickness relative to the chord line. Thickness is measured either perpendicular to the camber line or perpendicular to the chord line. The aerodynamic force created depends on the shape of the airfoil. The upper surface is related to high velocities and low static pressure and the lower surface has higher static pressure.

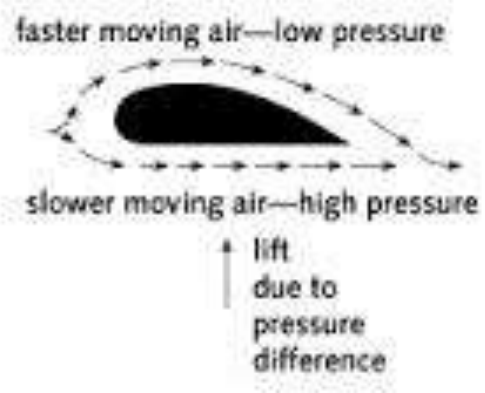

FIGURE 17. BASIC MODEL OF BERNOULLI PRINCIPLE

Figure 17 is a basic visualization of the Bernoulli Effect. The pressure difference can be calculated using Eq. (8), the Bernoulli equation. P_1 and P_2 is pressure, below and above the airfoil respectively, ρ is the density of the fluid, in this case air and V is the velocity of the fluid, g is gravity and h is the height from a specified axis.

$$P_1 + \frac{1}{2}\rho {v_1}^2 + \rho g h_1 = P_2 + \frac{1}{2}\rho {v_2}^2 + \rho g h_2 \tag{8}$$

When an airfoil is placed in a wind stream, its shape forces the wind over the upper camber to move faster causing low pressure. A possible explanation for this is the principle of conservation of mass. An important assumption is that the air is incompressible. Basically, the air flows over the foil in stream lines but the curvature at the top of the airfoil forces the streamlines closer together. Since the fluid flow must stay the same, the velocity above the foil must increases. The wind below the airfoil is slower with higher pressure. This produces a lift force due to the pressure difference. Figure 18 demonstrates this phenomenon using the airfoil cross-section we designed in this project.

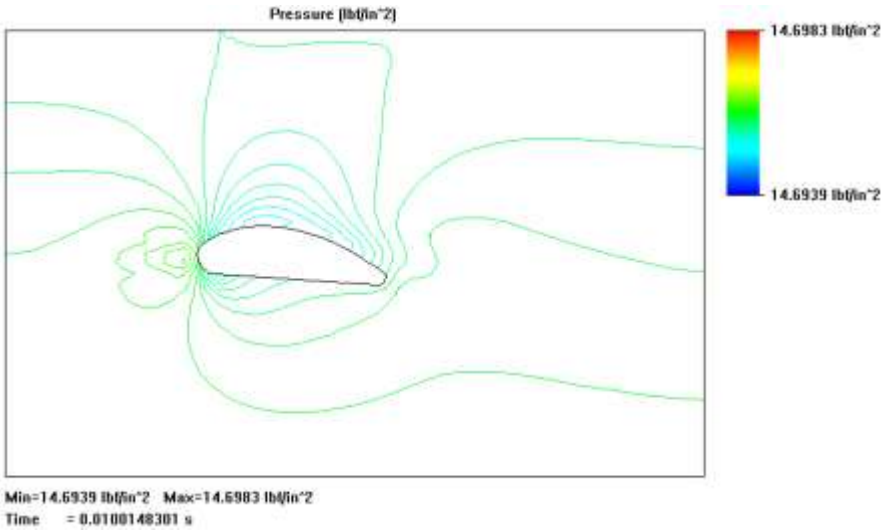

FIGURE 18. PRESSURE ISOLINES OVER OUR DARIEUS BLADE CROSS SECTION AS MODELED IN SOLIDWORKS

For obvious reasons, an airfoil shape that produces optimal lift is desired. An ideal symmetrical airfoil has a lift coefficient proven to be 2π times the angle of attack. Equation 9 is for a cambered airfoil. The lift coefficient must be adjusted by c_{L0} which is the lift coefficient when the angle of attack is zero.

$$c_L = c_{L0} + 2\pi\alpha \tag{9}$$

By looking at the Eq. 2, it is clear that a larger angle of attack can increase lift but it is limited by the shape of an airfoil. Also, the associated drag coefficient would increase. Upon analysis of multiple airfoils, the lift coefficients were approximately close to the theoretical value therefore, the drag coefficients were investigated. A few low drag airfoils often used in the design of Darrieus wind turbines are NACA 0012, NACA 0018 and NACA 4415. Per the naming conventions for NACA airfoils, in symmetrical airfoil names, the first digit is maximum camber as a percentage of the chord. The second digit describes the location of the maximum camber from the leading edge and the last 2 digits describe maximum thickness of the foil in relation to the coil. In airfoils with no camber, the first 2 digits are 0's. The ratings for each of the specifications including lift and drag coefficients for the selected airfoils are listed in Appendix A. Ultimately, we chose the NACA 4415 due to ease of manufacturing. It had a median thickness of the 3 and a larger camber.

After an airfoil shape was decided, we had to figure out how many blades would be most effective. Two or three blades are the standard but three blades were chosen because it resolves a few issues with vibrations, noise and starting.

Next we looked at the Tip Speed Ratio (TSR). Darrieus blades may spin several times faster than the wind. The tip speed ratio is the ratio of the tangential velocity of the blades to the wind velocity. The Tip Speed Ratio is one of the most important factors in the design of a wind turbine. Performance of a wind turbine is often modeled in a Cp versus Tip Speed Ratio curve such as that in fig. 20. If the blades are spinning too slowly, most of the wind will flow through the space between the blades however; if the blades are spinning too quickly it will be like wind flowing towards a solid wall. Having too many blades is not very effective and would require higher TSR's.

# of Blades		Optimum TSR
2	—	Around 6
3	—	Around 4—5
4	—	Around 3
6	—	Around 2

FIGURE 19. OPTIMUM TSR FOR A GIVEN NUMBER OF BLADES.

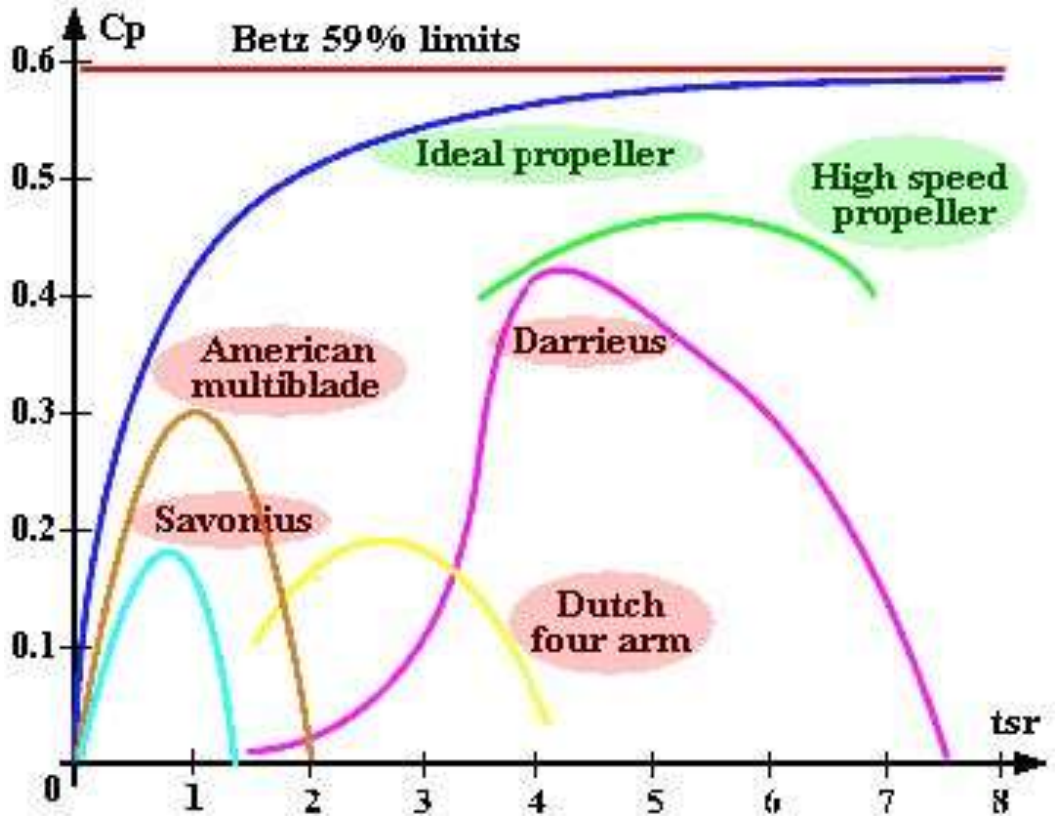

FIGURE 20. CP VALUES FOR GIVEN WIND TURBINES

Figure 20 shows the optimum Tip Speed Ratio for a given number of blades based on empirical data. The number of blades required has an inverse relationship to the optimum TSR. With a three blade configuration a tip speed ratio of about 4-5 is ideal.

The angular frequency of the Darrieus blades can be calculated using Eq. 10 wherein λ is the TSR and r is the radius of the turbine.

$$\omega_f = \frac{\lambda v}{r} \tag{10}$$

With a wind velocity of 5 mph or 134.11 meters per min, a radius of 18 inches and a tip speed ratio of 4, the angular frequency of the Darrieus blades is 186.7 rpm.

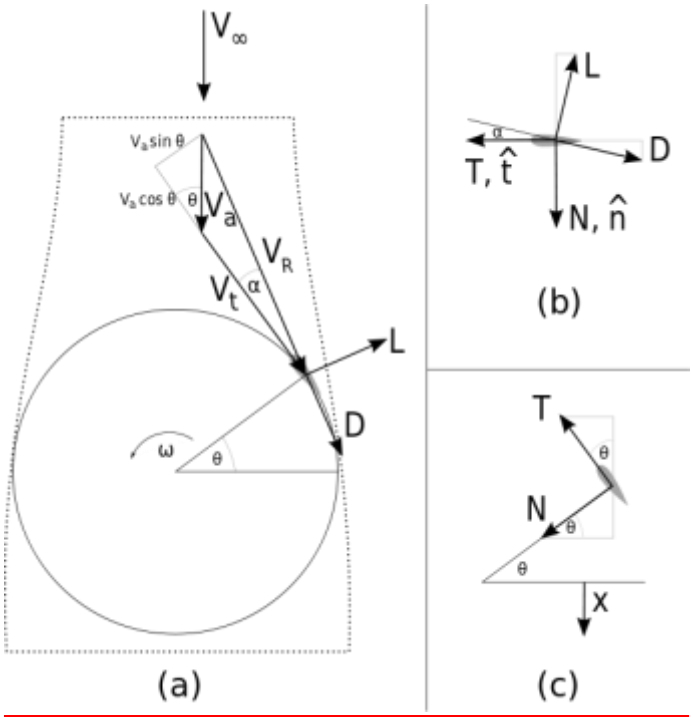

FIGURE 21. TOP VIEW OF A FORCE DIAGRAM FOR A DARRIEUS VAWT

Figure 21 is a force diagram showing the top view of a turbine blade on a Darrieus vertical access wind turbine. α is the angle of attack. The optimum angle of attack creates the maximum lift to drag ratio. An angle of attack between 1 and 15 degrees is desirable with the standard being about 4 degrees.

V_ω is the velocity of the wind. ω is the rotational velocity. L is the lift force and D is the drag force. T denotes the tangential force, and N denotes a normal force. θ is the angular position of the blade, which is also called the pitch angle. V_t opposes tangential velocity. x is the turbine axis. The drag force is parallel to the relative velocity and oriented in the same direction as the wind. The lift force is always perpendicular to the drag force and the relative velocity of the wind. The tangential velocity can also be called the tip

velocity and is calculated by multiplying the angular velocity of the turbine by the radius as in Eq. (11).

$$V_t = \omega R \tag{11}$$

The angle of attack is also important because it determines the blades orientation and it is a major influence on the torque exerted on the central column.

Additionally, the forces due to the drag force can be determined with equations 12 and 13. Lift and drag coefficients are found for the airfoils considered in Appendix A.

$$F_l = \frac{1}{2}\rho_{air} \times V^2 \times d_t \times bl \times C_l \tag{12}$$

$$F_d = \frac{1}{2}\rho_{air} \times V^2 \times d_t \times bl \times C_d \tag{13}$$

The equations for the lift force, F_l, and drag force, F_d, require the blade length, bl, lift coefficient C_l, and drag coefficient, C_d. At a 4 degree angle of attack, the lift coefficient for our blades is .9041 and the drag coefficient is .02134. This means there is a .34 lb lift force and very minor .008 lb drag force acting on the aerodynamic center of the blades.

We decided to add Savonius blades to improve the performance of the Darrieus blades. For our design we limited the size of the two cup scoops to fit within the radius of the Darrieus blades.

In a Savonius turbine the areas swept by the turbine is given by Eq. (14).

$$A_s = h_s r_s \tag{14}$$

In eq. (14) h and r are the height and radius of the rotor respectively. In a Savonius rotor the TSR =1. With a radius of 13.5 inches and a height of 19 inches, the area swept by the Savonius blades is 256.5 in^2.

Therefore, the angular frequency calculated using equation 10 is about 70 rpm. This will slow down the Darrieus blades.

The design calls for Savonius blades between 12 and 20 inches in diameter.

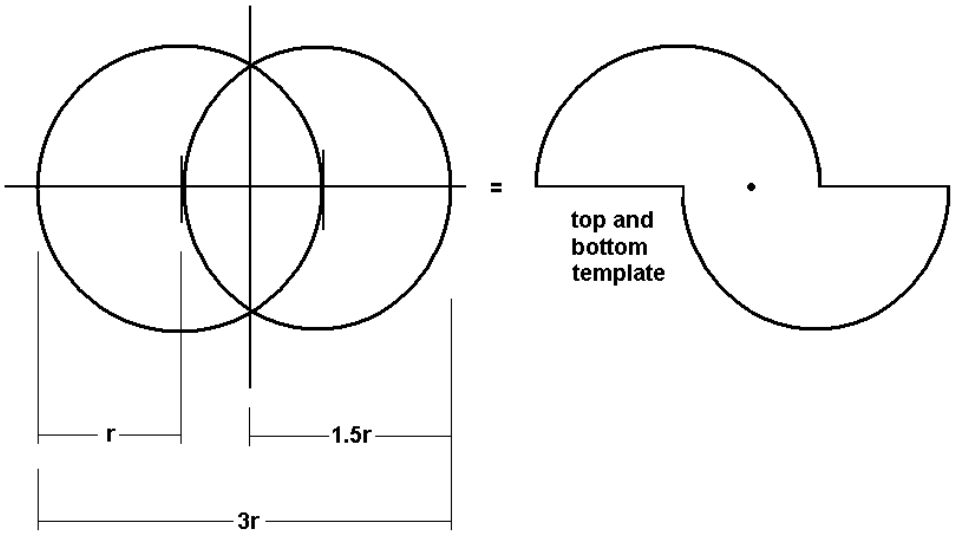

FIGURE 22. CONFIGURATION OF SAVONIUS SCOOPS

The Savonius scoops must be configured such as in Fig. 22. The cylinders will be cut in half and one is offset to the center line. In this manner, air entering through one half of a scoop will be recycled to the scoop attached to it on the opposite side. Additionally, a second pair of scoops can be stacked on top of the first pair and placed at 90 degrees to avoid the turbine stalling in a certain position.

This greatly increases the efficiency of the Savonius components.

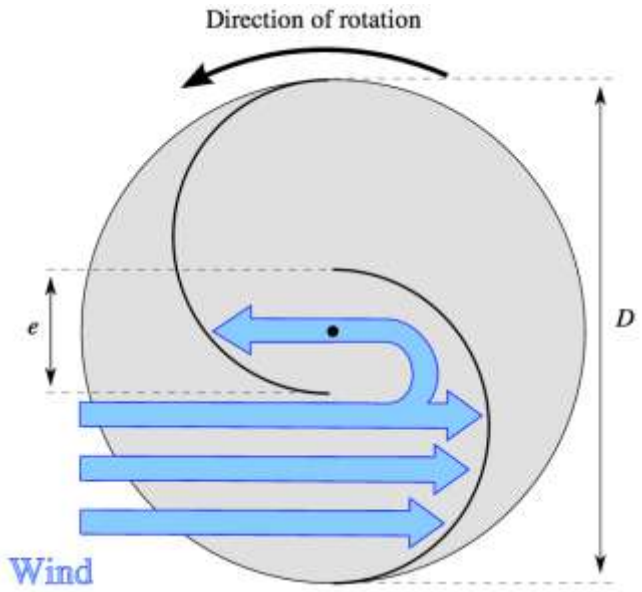

FIGURE 23. FLUID FLOW THROUGH SAVONIUS ROTOR

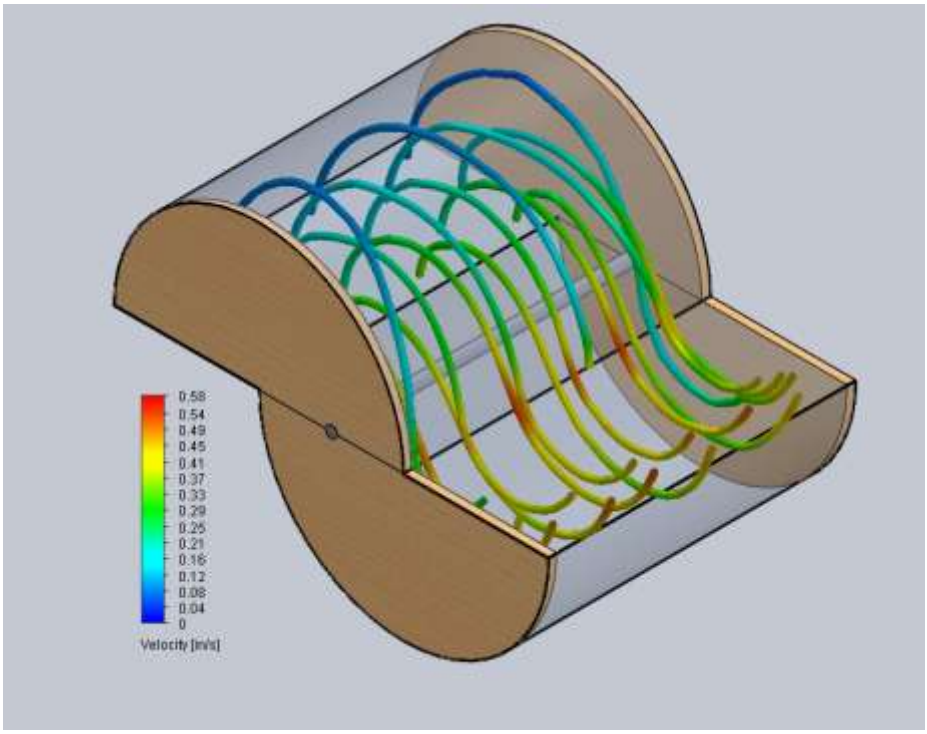

FIGURE 24. SOLIDWORKS SIMULATION OF FLUID FLOW THROUGH THE SAVONIUS ROTOR

Using Solidworks, it was possible to model the fluid flow through our designed Savonius rotor. Once again the importance of offsetting the hemispheres by 1 radius was

demonstrated. As the fluid flows through the inlet, it bounces off the wall and escapes through the outlet. This fluid analysis was completed after the prototype was built confirming the theory.

Both the Savonius and the Darrieus blades needed to be made of durable lightweight material. Fiber glass, balsa wood and thin metal sheets were considered for the design of the Darrieus blades. Originally, PVC pipe was considered for the Savonius but the wall thickness for an appropriate diameter was much higher than anticipated. We were looking for a hollow lightweight cylindrical object for these blades.

STRUTS

Struts are used to attach the Darrieus blades to the collar. They had to be lightweight yet resistant to deformation. We decided to use 3/8 in aluminum rods and thread the ends. The maximum stress concentration would therefore be in the thread, therefore we used equations.

Equation 15 and Eq. (16) are used to calculate the body shear stresses due to the moment from torque at the exterior of the screw body and the axial normal stress respectively. The body shear stresses due to the torsional load for our struts are 16.7 Mpa and the axial normal stress is .097 Mpa.

$$\tau = \frac{16T}{\pi {d_r}^3} \tag{15}$$

$$\sigma = \frac{F}{A} = \frac{4}{F\pi {d_r}^2} \tag{16}$$

Empirical data suggest that the first thread amongst the engaged threads will carry a greater portion of the load. This is about .38F. The bearing stress with one thread carrying .38F can be calculated using Eq. (17). The bearing stress on our selected screws is .296 MPa.

$$-\sigma B = \frac{F}{\pi d_m n_t\, p/2} = -\frac{2F}{\pi d_m n_t\, p} \tag{17}$$

The thread root bending stress with one tooth carrying .38F is given by Eq. (18). The thread root bending stress was .8597 MPa.

$$\tau = \frac{3V}{2A} = \frac{3F}{2\pi d_r n_t\, p/2} = \frac{3F}{\pi d_r n_t\, p} \tag{18}$$

There is a transverse shear stress at the center of the thread due to the loading but the transverse stress at the top of the thread root due to bending is 0. The calculated normal and shear stresses are arranged in table 1.

TABLE 1. 3 DIMENSIONAL STRESSES ON THE SCREW.

Calculated 3 Dimensional Stresses			
σ_X	.8597 Mpa	τ_{XY}	0.0
σ_Y	-.0197 Mpa	τ_{YZ}	16.5 Mpa
σ_Z	0.0	τ_{ZX}	0.0

To find the von Mises stresses, principle stresses must be calculated using Eq. (19).

$$\sigma 1, \sigma 2 = \frac{\sigma x + \sigma y}{2} \pm \sqrt{\left(\frac{\sigma x - \sigma y}{2}\right)^2 + {\tau_{xy}}^2} \tag{19}$$

Once the three principle stresses were found they were rearrange in descending order to calculate the von Mises stress $'$ in Eq. (20) and τ in Eq. (21).

$$\sigma' = \left(\frac{(\sigma 1 - \sigma 2)2 + (\sigma 2 - \sigma 3)2 + (\sigma 3 - \sigma 1)}{2}\right)^{1/2} \quad (20)$$

$$\tau_{max} = \frac{\sigma 1 - \sigma 3}{2} \quad (21)$$

The maximum normal stress on the screws due to loading is 28.93 Mpa and the maximum shear stress due to the specified loading is 20.7 Mpa. A safety factor was calculated using Eq. (22).

$$n = \frac{Sy}{6} = 7 \quad (22)$$

COLLAR

A custom collar was designed to attach the three Darrieus blades to the shaft. Figure 24 shows the custom designed collars.

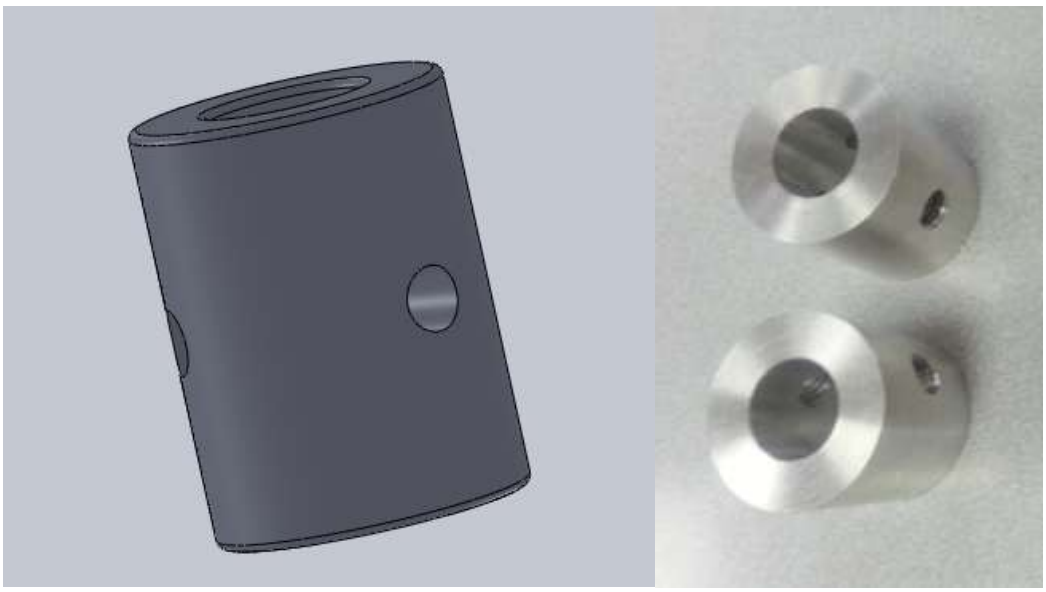

FIGURE 24. COLLAR FOR DARRIEUS BLADES.

The collar fits snugly around the shaft with 3 threaded holes evenly spaced around its center. One end of each of the three rods will be threaded through the collar and shaft. The other end of the rods will be threaded and bolted to the blades.

Aluminum Unthreaded Spacers

Aluminum

Also called clearance spacers. They have an OD tolerance of ±0.005", ID tolerance of +0.01", and length tolerance of ±0.005".

CAD For technical drawings and 3-D models, click on a part number.

Screw Size	ID
3/4"	0.755"
1"	1.005"

		Aluminum	
			Each
Lg.	Available Screw Sizes		1-9	10-Up
1 1/2" OD				
1 1/2"	3/4", 1"	92510A374	$12.15	$10.32

FIGURE 25. SPACER CONSIDERED FOR THE DESIGN OF THE COLLAR.

In order to decrease manufacturing time and cost we debated on purchasing a spacer with the appropriate outer and inner diameter and machining the three threaded holes. Figure 25 shows the specifications for the spacer considered. We were able to purchase a solid piece of aluminum 2 inches in diameter and 6 inches long. We outsourced the manufacturing of the collar. In this case, the maximum stress concentration should also be on the threads, a SolidWorks model was used to model stress in the collar.

SHAFT

The shaft is integrated into the system to transmit power from the prime mover, which in this case are the rotating blades to the generator. The shaft is made from ¾ inch stainless steel. Each Darrieus blade will be mounted to two 3/8 inch aluminum struts, which are in turn mounted to the collars. The three equally spaced threaded rods are threaded at both ends and meet in the center of the rod. The Savonius blades are also

attached to the central column as well as the bearings and a gear. Two bearings are placed on either side of the gear for stable support and well balanced loading of the bearings.

The shaft will experience a combination of normal, torsional shear and bending stresses from the applied loads. The distortional energy theory of failure was utilized to analyze the shaft.

With a wind velocity of 5 mph the angular velocity of the turbine is 128 rpm from the average of the Darrieus and Savonius blades.

The total torque on the central column can be found using the known output power and angular velocity as in Eq. (23).

$$T = \frac{P}{\omega} \tag{23}$$

Therefore the total torque on the central column is about .06 N*m when the turbine is rotating at 150 rpm.

TABLE 2. TESTED TORQUE CALCULATIONS BASED ON POWER OUTPUT AND RPM

RPM	Volts	Current	Watts	Kwh	Torque
561	5.33	0.6625	3.511	0.14	0.059793
465	4.6	0.575	2.645	0.105	0.054345
260	2.68	0.335	1.54	0.06	0.056589
152	1.75	0.22	1.011	0.04	0.063547

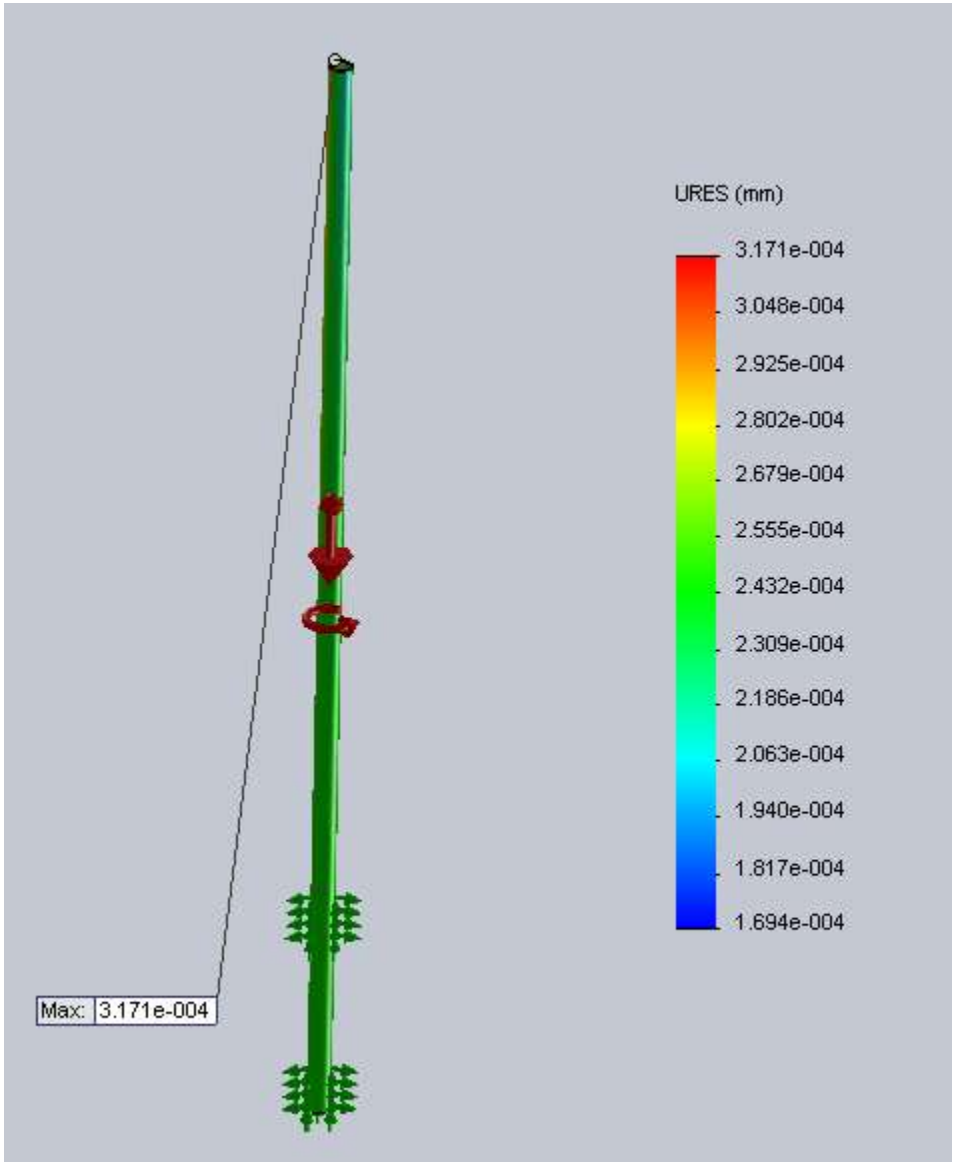

FIGURE 26. DISPLACEMENT ON THE CENTRAL COLUMN

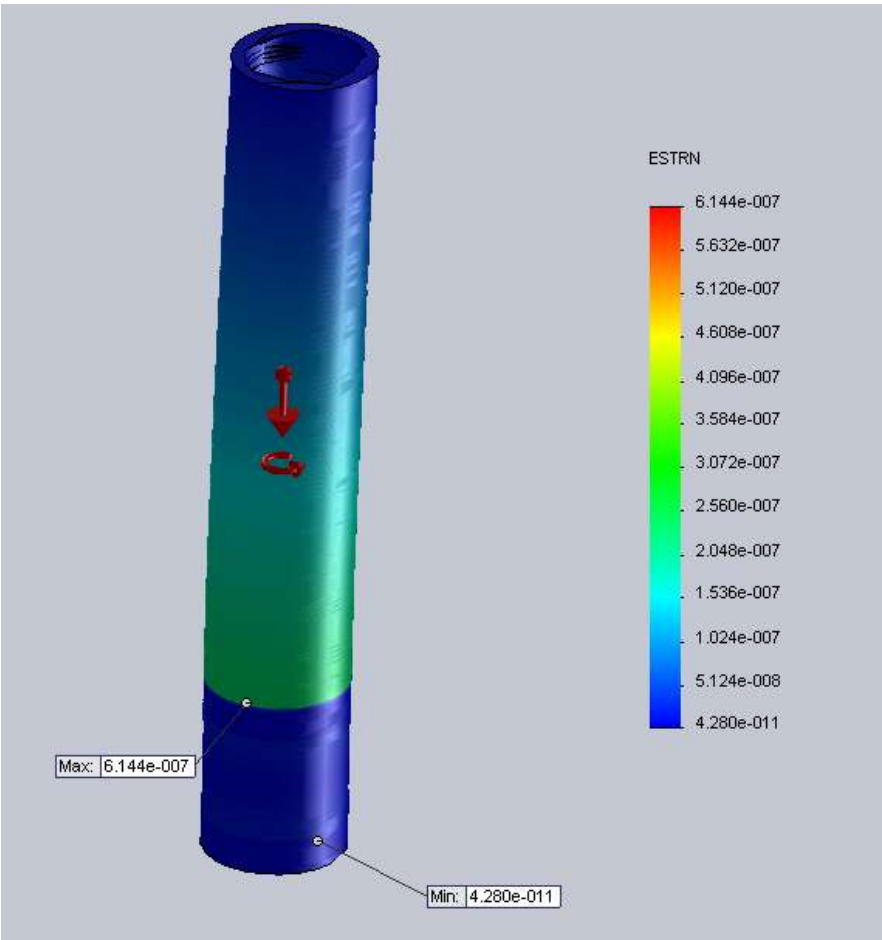

FIGURE 27. STRAIN FOR A HIGHWAY WIND TURBINE

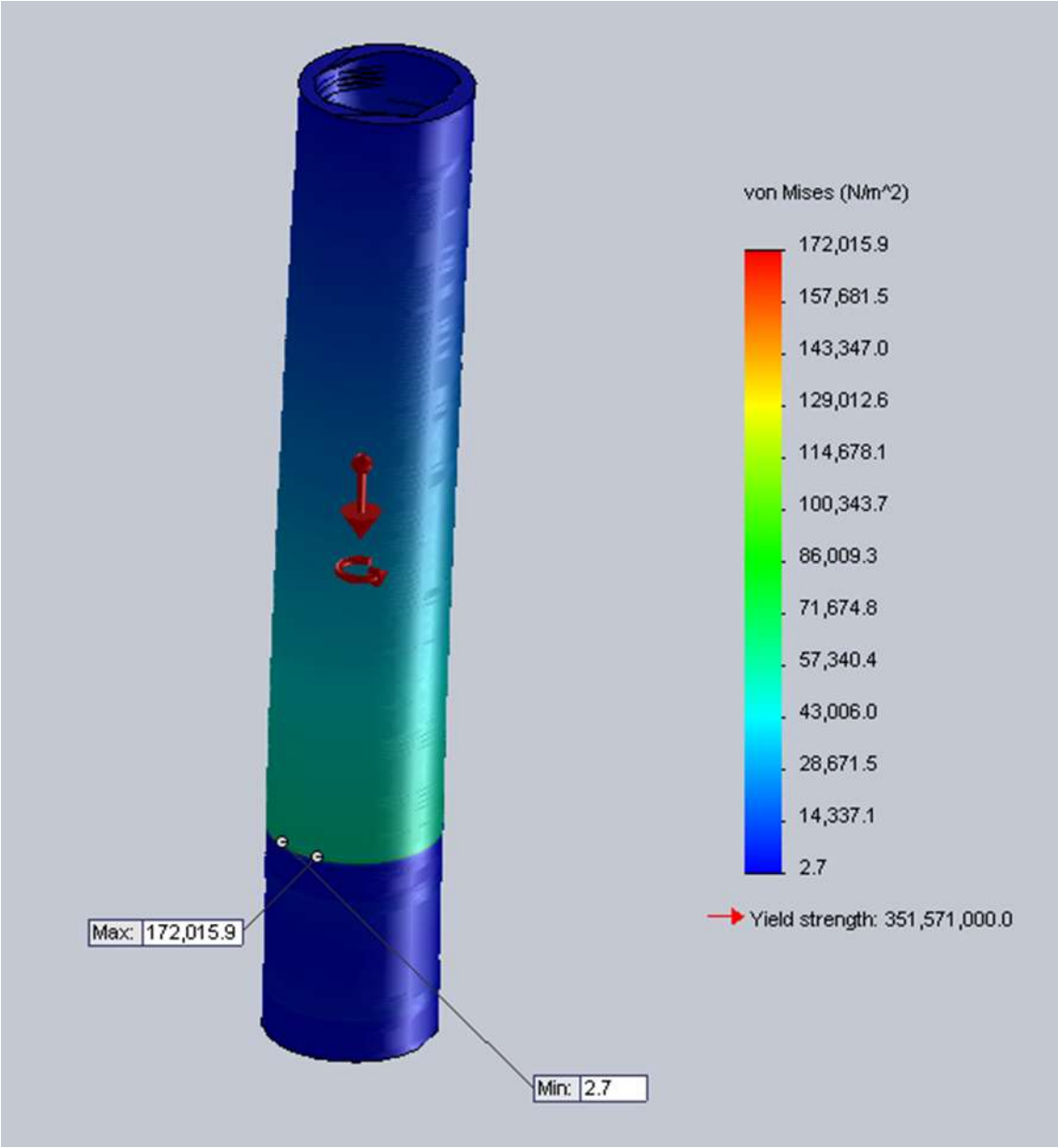

FIGURE 28. VON MISES STRESSES ON THE SHAFT

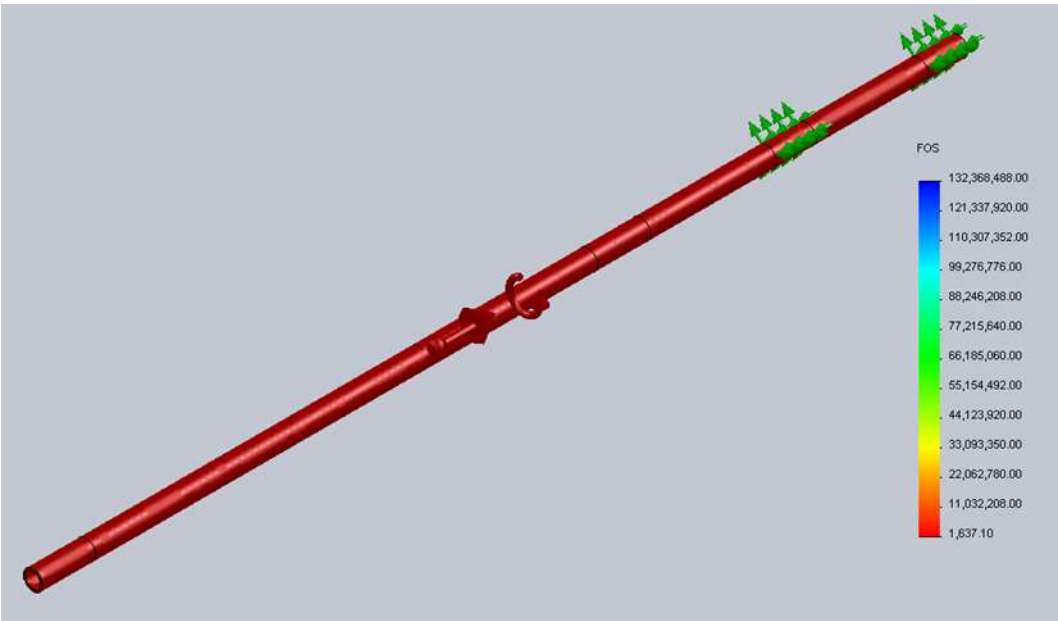

FIGURE 29. FACTOR OF SAFETY

The simulation in fig. 28 yielded values of172 $KPa\ MPa = \sigma_{vm}$. The next step shown is a calculation for the factor of safety using the equation (24).

$$\frac{S_y}{n} = \sigma_{vm} \tag{24}$$

The factor of safety for our shaft is 1637.

BEARINGS

For our bearing selection we started with the dimensions that best suited our design. The dimension desired was a .75 inch diameter to fit the shaft. We found a bearing with these dimensions shown in Fig. 30.

Figure 30. Bearing selected with specifications

Next, we checked if the load rating on this bearing is enough to support our design load needs. The dynamic load rating is 193 lbs on McMaster-Carr; the static loading is much less. To find our loading needs we started with some known parameter shown in table 7.

TABLE 3. KNOWN PARAMETERS FOR DYNAMIC LOAD CALCULATION

Fa	13.5	Axial load [lbf]	Xo	0.02	Assumed Weibull parameter
Fr	4.3	Radial load [lbf]	Sigma	4.459	Assumed Weibull parameter
V	1	Inner ring rotates	af	1.2	Application factor
R	0.9	Reliability	a	3	Roller bearing parameter
n	150	Speed [rpm]	b	1.483	Roller bearing parameter
Co	6.2	Static load rating [lbf]	C10	12.7	Dynamic load rating [lbf]

Other parameter needed was the equivalent load (Fe) in Eq. (25).

$$Fe = XiVFa + YiFr \tag{25}$$

To solve this equation we needed the values for X and Y. the first step was to calculate $^{Fa}/_{Co}$ to get a value "e" and then compare e to $^{Fa}/_{(VFr)}$ and using Fig. 31 we were able to get the values for X and Y. If $^{Fa}/_{Co}$ is less than .014, the instructions are to use the values for .014.

		$F_a/(VF_r) \le e$		$F_a/(VF_r) > e$	
F_a/C_0	e	X_1	Y_1	X_2	Y_2
0.014*	0.19	1.00	0	0.56	2.30
0.021	0.21	1.00	0	0.56	2.15
0.028	0.22	1.00	0	0.56	1.99

FIGURE 31. X AND Y VALUES TO DETERMINE FE

We determined $Fa/_{Co}$ yielding an e of .19, and $Fa/_{(VFr)}$ was 3.14. We were able to determine we could use X2 and Y2, because $Fa/_{(VFr)} > e$, as shown in fig. 31. The value of X2 used was 0.56 and for Y2 it was 2.30. Using Eq. 26 Fe was determined to be 17.45 lbf.

The final needed value needed wasX_D. Eq. (26) was used.

$$X_D = \frac{60\mathcal{L}_D n_D}{10^6} \tag{26}$$

The $\mathcal{L}_D$ was rated for 100,000 hours (about 10 years). With these parameters we can solve Eq. (27) for the dynamic load rating of our design.

$$C_{10} = a_f F_e \left[\frac{x_D}{x_0 + (\theta - x_0)(1 - R_D)^{\frac{1}{b}}}\right]^{\frac{1}{a}} \tag{27}$$

The value yielded by Eq. 28 for the dynamic loading needed to support our design was 7.3 lbf. The catalog dynamic load this bearing can sustain 28.18 lbf which is easily above our design needs, making this bearing a suitable one for our design.

MOTOR

The gears, generator, battery and other components were bought and are housed at the base of the turbine. The main consideration for the motor is that it requires very low rpm's to produce a high voltage. The challenge was that the angular frequency is inversely proportional to the torque. The base is not shown in the SolidWorks model however, it will

be attached to the shaft using the bearings in figure 35. Once the turbine is designed, a gearbox may be designed to step up the power output.

FIGURE 32. GENERATOR SELECTED

TABLE 4. MANUFACTURER RATINGS FOR PERMANENT MAGNET ALTERNATOR

RPM	VOLTS	AMPS
150	12	1.5
300	25	4
500	43	7
750	60	10
1000	70	11

The generator selected is a permanent magnet alternator. According to the manufacturer, the generator can produce 12 volts with 150 rpm. We tested the generator and determined that the motor can indeed produce 12 volts at fewer than 150 rpm however; it requires a large torque to get started. It is recommended that

GEARS

Most turbines have gearboxes to "step-up" the angular velocity of the turbine. This is particularly important in the design of the highway wind turbine because it is placed at lower elevations with slower moving wind. With a wind speed varying between 0 and 8 miles per hour, we calculated that the shaft would be rotating an average of… rpm.

To amplify the number of rotations, we used a simple gear train consisting of 2 gears. Initially, we wanted to produce the maximum ratio of 10 with one set of gears however, it would run the risk of interference.

We chose gears to achieve a gear train value of 10 using Eq. (28).

$$e = \frac{product\ of\ driving\ tooth\ number}{product\ of\ driven\ tooth\ number} \tag{28}$$

The minimum amount of teeth on the pinion necessary to avoid interference is given by Eq. (29). With a pressure angle of 20 degrees we calculated the minimum amount of teeth for a gear ratio of 10 was 17. Therefore, we would have to get a pinion gear with 17 or more teeth and a mating gear with 10 times as many teeth. We found that gears that large were a little more expensive than we planned for. It was also difficult to find a coordinating pair of gears with those specifications.

$$\mathrm{Np} = \frac{2k}{(1+2m)sin^2\theta}(m + \sqrt{m^2 + (1+2m)sin^2\theta} \tag{29}$$

We ultimately found a set of gears to produce a gear train value of 5. The two gears selected have a 14.5 degree pressure angle, with a ¾ in face width and 12 in pitch. The pinion gear is made of high strength steel whereas the mating gear is made of cast iron.

FIGURE 33. PINION AND MATING GEAR.

For a pressure angle of 20 degrees, this set of gears would have been acceptable, however when the pressure angle was changed to 14.5 in a template created specifically for this analysis, the minimum number of teeth was 30. We already purchased the gears but in future designs, we will address this problem.

The pinion would receive the velocity from the shaft at about 130 rpm and using the train value from Eq. (13) the mating gear would rotate at 650 rpm.

Figures 33 and 34 are force diagrams for each of the selected gears in our gear design.

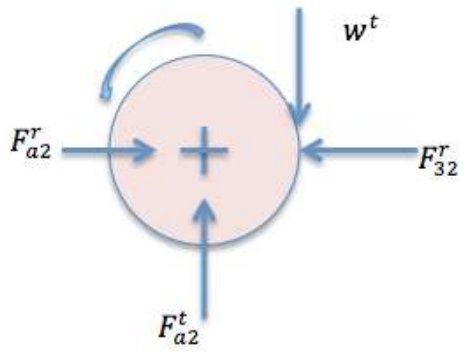

FIGURE 34. PINION, GEAR 2, FREE BODY DIAGRAM

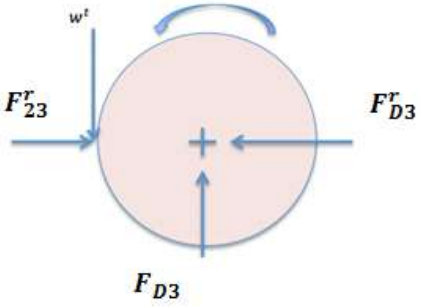

FIGURE 35. MATING GEAR FREE BODY DIAGRAM

To determine stresses involved in the gears, first we found tangential load and pitch velocity using table 6.

TABLE 5. PITCH VELOCITY AND TANGENTIAL LOAD

$V = \frac{\pi D_p n}{12}$	$43.44 \frac{ft}{min}$
$w^t = \frac{33000H}{V}$	1.255 lbf

The analysis was done at the pinion only. The pinion had the least amount of teeth and the lowest pitch diameter which made it more susceptible to failure than the mating gear. The bending stress in the pinion gear due to bending is given by the Lewis Bending Equation, Eq. (30).

$$\sigma_B = W^t K_v \frac{P_d}{FY} \tag{30}$$

The safety factor for the allowable stress due to bending in the model is given by Eq. (31)

$$S_f = \frac{S_t Y_N / K_t K_R}{\sigma_B} \tag{31}$$

The stress in the gears due to contact is given by Eq. (32)

$$\sigma_c = C_p \left(W^t K_v K_s \frac{K_m}{D_p F} \frac{C_f}{I} \right)^{\frac{1}{2}} \tag{32}$$

The safety factor for the allowable stress due to contact in the model is given by Eq. (33).

$$S_H = \frac{S_c Z_N C_H / (K_t K_R)}{\sigma_c} \tag{33}$$

We had to make several assumptions in order to determine the safety factor. Wt and V calculations are shown in table 5. The specifications sheet for the gears stated the material was high carbon steel; we used a very conservative Brinell Hardness of 160. This HB value was used for the calculation of St and Sc. For a steel pinion mating with a cast iron gear, the elastic coefficient Cp is 2100. For YN and ZN life cycles were assumed at 10^7based on

AGMA standards. Finally, the geometry factor was calculated in Eq. (33) where $m_N = 1$ for spur gears and m_G is the ratio between the pinion and mating gear, 5.

Equation 34 is used to calculate the dynamic effect coefficient for Cut or milled profile.

$$Kv = \frac{1200 + V}{1200} \tag{34}$$

Equation 35 is used to calculate allowable bending stress number.

$$Grade\ 1$$

$$St = 77.3\,HB + 12\,800\,psi \tag{35}$$

Contact fatigue strength can be calculated using Eq. (36).

Grade 1

$$Sc = 322\,HB + 29\,100 psi \tag{36}$$

Stress cycle factors for life cycles at 10^7 were calculated using Eq. (37) and (38).

$$YN = 1.6831\,N^{-0.0323} \tag{37}$$

$$ZN = 2.466\,N^{-0.056} \tag{38}$$

Equation 39 was used to calculate the geometry factor of pitting resistance for external gears.

$$I = \frac{cos\,\varphi t\ sin\,\varphi t}{2mN}\frac{mG}{mG + 1} \tag{39}$$

TABLE 6. VALUES FOR STRESS AND FACTOR OF SAFETY CALCULATIONS

Pinion

Kv	1.01	St	25168
Wt	4.45	Yn	0.928
V	1.06	Sc	80620
Y	0.29	Zn	0.879
HB	160	Cp	2300
Life	100000000	I	0.113

The assumptions of some "k" values to be equal to 1 reduced the equations. The calculated stress factors and factors of safety for the design are listed in table 7.

TABLE 7. BENDING AND CONTACT STRESSES AND SAFETY FACTORS

$\sigma_b = \frac{k_v w^t P}{F_d Y}$	4080 Psi	SF=$\frac{S_t Y_n}{\sigma_b}$	5.72
$\sigma_c = C_p \sqrt{\frac{w^t k_v}{D_p F I}}$	52293 Psi	SH=$\frac{S_c Z_n}{\sigma_c}$	1.36

Table 8 shows the safety factor due to contact was 1.36 while the safety factor for bending was 5.72. All of the values calculated were for the pinion which means the mating gear is safe as well.

SYSTEM DYNAMICS MODELING

Our VAWT is a combination of different systems and allows conversion of kinetic energy from the wind into electrical energy. The wind from passing vehicles enables mechanical rotation of the blades which then produces a torque on the gears. The gear system allows the generator to convert the mechanical energy to electrical energy. The energy is then amplified by a transformer and output to a streetlight. System dynamics modeling is used to illustrate the state of the system over a given time period.

SYSTEM GRAPH

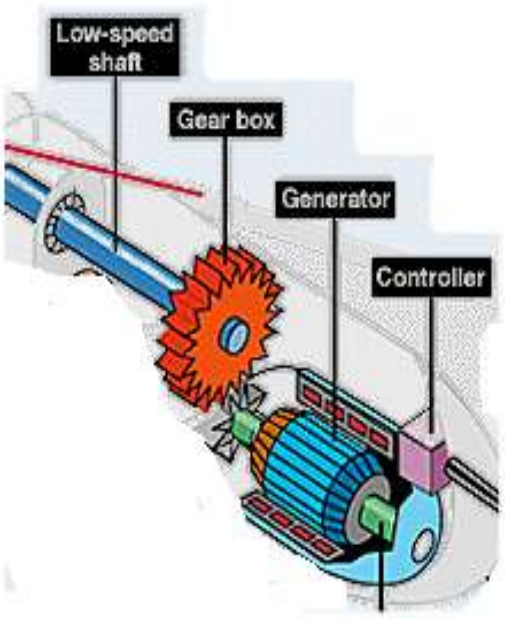

FIGURE 36. INSIDE VIEW OF A TYPICAL WIND TURBINE

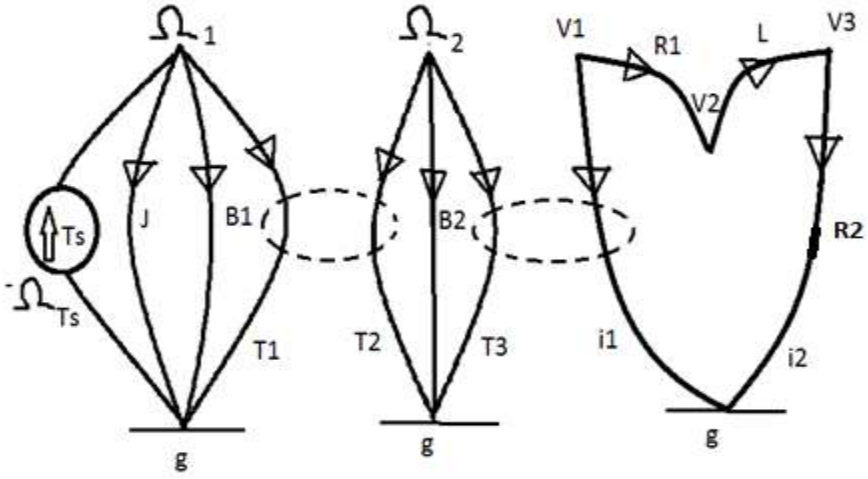

FIGURE 37. SYSTEM GRAPH

Figure 21 is a visualization of the 4 systems utilized in the VAWT. The first part is the turbine blades which receive an input torque related to the wind that is connected to the gearbox (part 2) which changes the angular velocity. It is converted to an electrical system with the generator (part 3).

b=11, s = 1, n = 8, p = 3

where b represents the number of branches, s represents the number of sources, n represents the number of nodes and p represents the number of parts.

ELEMENTAL EQUATIONS: B - S = 11 – 1 = 10

$T_j = J\frac{d\Omega_{1g}}{dt}$

$T_{b1} = b_1\Omega_{1g}$

$T_1 = N_G T_2$

$\Omega_{1g} = -\frac{1}{N_G}\Omega_{2g}$

$T_{b2} = b_2\Omega_{2g}$

$V_{1g} = K_{v_{1g}}\Omega_{2g}$

$i_1 = -\frac{1}{K_{v1g}}T_3$

$i_{R_1} = \frac{1}{R_1}V_{12}$

$\frac{di_L}{dt} = \frac{1}{L}V_{23}$

$i_{R_2} = \frac{1}{R_2}V_{3g}$

NODAL EQUATIONS: N – P = 8 – 3 = 5

$T_s = T_j + T_{b1} + T_1$

$T_2 + T_{b2} + T_3 = 0$

$i_1 = i_{R_1}$

$i_{R_1} = i_L$

$i_L = i_{R_2}$

CONTINUITY EQUATIONS: B – (N – P) = 10 – (8 – 3) = 5

$-\Omega_{Ts} + \Omega_{1g} = 0$

$-\Omega_{1g} + \Omega_{1g} = 0$

$-\Omega_{1g} + \Omega_{1g} = 0$

$-\Omega_{2g} + \Omega_{2g} = 0$

$-V_{1g} + V_{12} + V_{23} + V_{3g} = 0$

Source: T_s

STATE VARIABLE EQUATIONS:

$\dot{\Omega}_{1g} = \frac{T_j}{J} = \frac{1}{J}[T_s - T_1 - T_{b1}] = \frac{1}{J}[T_s - (b_1\Omega_{1g}) - T_1]$

$T_1 = N_g T_2 = N_g [- T_3 - T_{b2}]$

$T_1 = N_g [- T_3 - (b_2\Omega_{2g})]$

$T_1 = N_g [- T_3 - [b_2(- N_G\Omega_{1g})]$

$T_1 = N_g [- (-i_1 K_{v_{1g}}) + (b_2 N_G\Omega_{1g})]$

$T_1 = N_g [(i_{R_1} K_{v_{1g}}) + (b_2 N_G\Omega_{1g})]$

$T_1 = N_g [i_L K_{v1g} + (b_2 N_G\Omega_{1g})]$

$\dot{\Omega}_{1g} = \frac{1}{J}[T_s - (b_1\Omega_{1g}) - N_g [i_L K_{v_{1g}} + (b_2 N_G\Omega_{1g})]$

$\dot{I}_L = \frac{1}{L} V_{23} = \frac{1}{L} [-V_{3g} - V_{12} + V_{1g}] = \frac{1}{L} [-V_{3g} - V_{12} + (K_{v_{1g}}\Omega_{2g})]$

$$= \frac{1}{L}[-V_{3g} - V_{12} - K_{v_{1g}} N_G \Omega_{1g}]$$

$$= \frac{1}{L}[-V_{3g} - (i_{r1} R_1) - K_{v1g} N_G \Omega_{1g}]$$

$$= \frac{1}{L}[-V_{3g} - (i_L R_1) - K_{v1g} N_G \Omega_{1g}]$$

$$\dot{I}_L = \frac{1}{L}[-(i_{R_r} R_2) - (i_L R_1) - K_{v_{1g}} N_G \Omega_{1g}]$$

$$\dot{I}_L = \frac{1}{L}[-(i_L R_2) - (i_L R_1) - K_{v_{1g}} N_G \Omega_{1g}]$$

$$\begin{bmatrix} \dot{\Omega}_{1g} \\ \dot{I}_L \end{bmatrix} = \begin{bmatrix} -\frac{(b_1 + N_G{}^2 b_{2)}}{J} & \frac{-N_G K_{V1g}}{L} \\ \frac{-K_{V1g} N_G}{J} & -\frac{(R2+R_1)}{L} \end{bmatrix} \begin{pmatrix} \Omega_{1g} \\ I_L \end{pmatrix} + \begin{bmatrix} 1 \\ 0 \end{bmatrix} * (T_S)$$

The angular velocity of the blades and the inductance in the motor are the state variables.

INPUT VARIABLES

The source Torque (Ts) in the state variable equation is directly related to the velocity of the wind. We will be varying this input according to the equation:

A + B sin(omega*t)

where A is the amplitude of the source strength and B is the variation in the source strength and omega is the frequency of the variation. We used this equation to simplify the model because velocity of the turbine will not always be constant but may vary between 0 to as much as 12 mph. In the system analysis, the amplitude of source strength A is 5, we used a value of .7 for the frequency of variation and a value of pi.

In order to solve the state variable equations the Runge Kutta 4th order numerical method was utilized.

$$\dot{y} = f(t, y), \quad y(t_0) = y_0.$$

$$y_{n+1} = y_n + \tfrac{1}{6}h\left(k_1 + 2k_2 + 2k_3 + k_4\right)$$
$$t_{n+1} = t_n + h$$

$$k_1 = f(t_n, y_n),$$
$$k_2 = f(t_n + \tfrac{1}{2}h, y_n + \tfrac{h}{2}k_1),$$
$$k_3 = f(t_n + \tfrac{1}{2}h, y_n + \tfrac{h}{2}k_2),$$
$$k_4 = f(t_n + h, y_n + hk_3).$$

FIGURE 38. 4TH ORDER RUNGE KUTTA CONFIGURATION

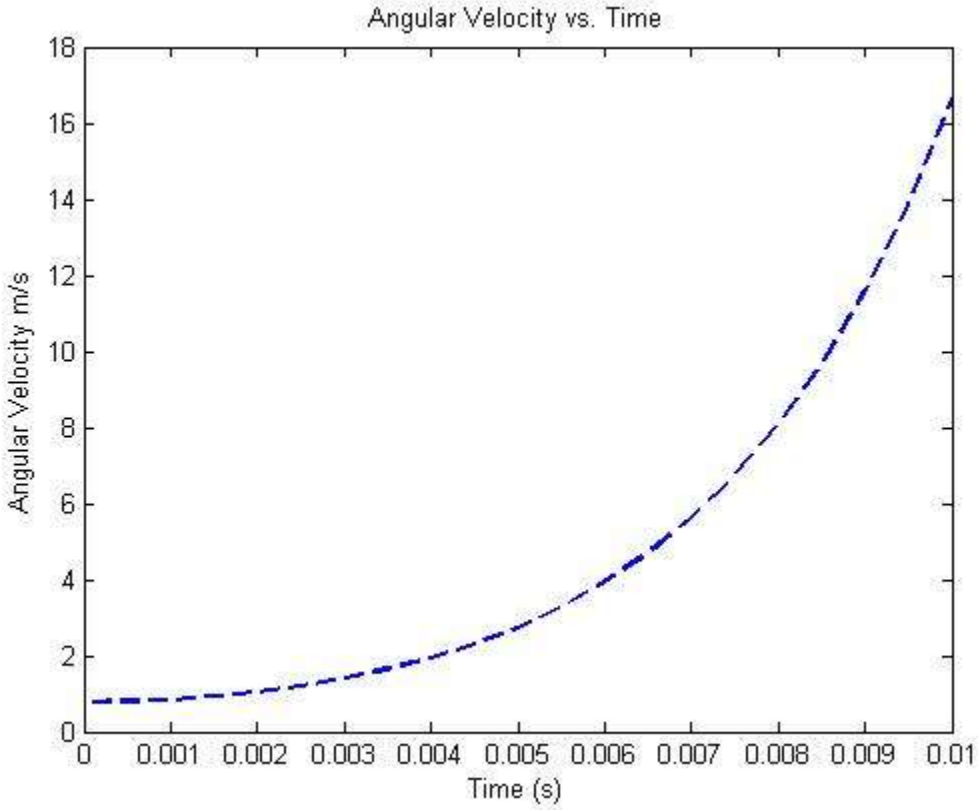

FIGURE 39. ANGULAR VELOCITY OVER TIME

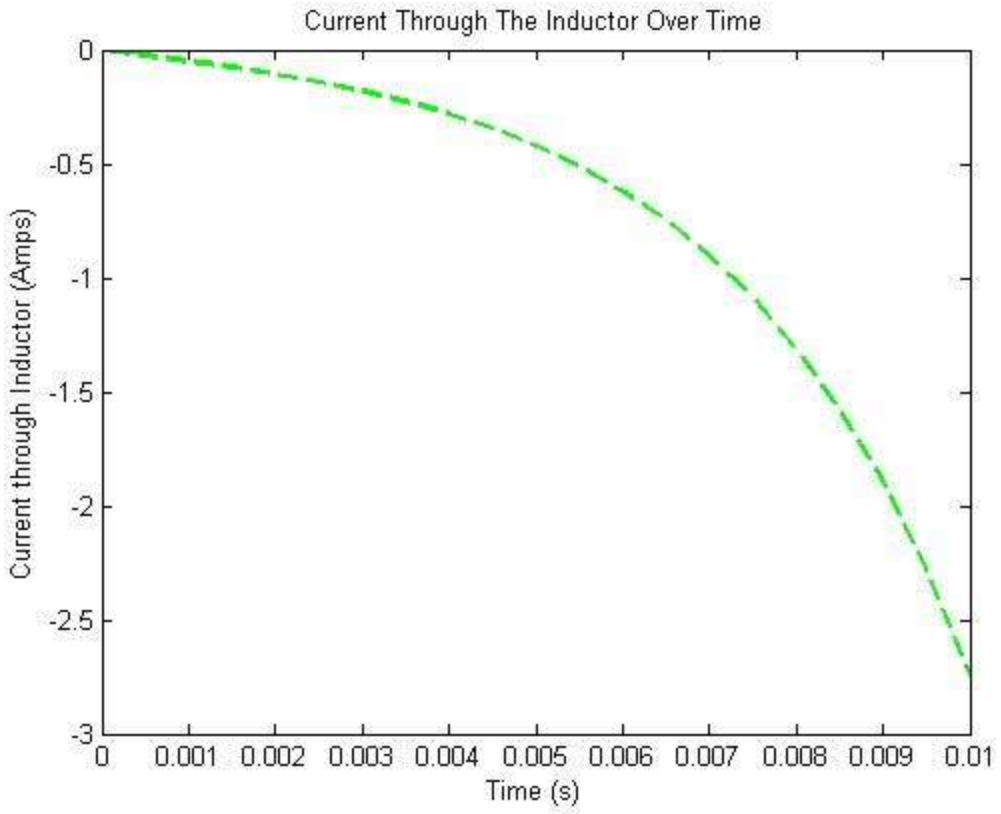

FIGURE 40. CURRENT THROUGH INDUCTOR OVER TIME

Figure 38-40 illustrates the use of MatLab to solve the matrix at different instances in time. Also the parameters that were used for the different components of the system being analyzed can be seen.

The 4th order Runge Kutta method was utilized to solve the simultaneous differential equations from the two state variables. The complete MatLab code for these calculations is in appendix B. An approximation of angular velocity and the current through the inductor was found for each .001 second increment in time. From the results, the angular velocity is increasing almost exponentially with time and the current through the inductor is decreasing over time. This means that the voltage in the inductor is pushing positive charge in the direction of current to oppose the decrease.

COST ANALYSIS

We do not have a sponsor for this project therefore the costs is divided among group members. Average costs of some turbine parts are listed. Figure 11 shows average costs of several of the major components in a vertical wind turbine. To reduce costs, some of the components will be manufactured such as the wind turbine blades.

According to data collected, the rotor and blades typically comprise about 20% of turbine costs. The generator is the most expensive component with a 34% share of total costs and the frame is about 15% of the total manufacturing costs.

Part	*Part Description*	*Source*	*Quantity*	*Price/Part*	*Totals*
Shaft	Crown Bolt 36 in. x 3/4 in. x 1/16 in. Plain Steel Round Tube	Home Depot	1	$9.32	$9.32
Collar	Aluminum Unthreaded Spacers		2	$22.50	$45.00
Wood	1/2 inch and 3/4 inch thick plywood		1	$60.00	$60.00
Threaded Rods	3/8 in rod aluminum (we threaded the ends)		6	$2.87	$17.22
Aluminum Sheets	for Blades		3	$68.40	$205.20
Generator	12 Volt 150 RPM Permanent Magnet Alternator	Ebay	1	$156.00	$156.00
Gears	Set of 1 90 teeth gear and 1 18 teeth, .75 FW, 14.5 P.A.		1	$1.22	$1.22
Bolts and nuts	3/8x16		8	$1.19	$9.52
				Total	$503.48

FIGURE 41. COSTS OF VERTICAL WIND TURBINE COMPONENTS

PROTOTYPE DESIGN AND TESTING

MATERIAL SELECTION

We used steel in the shaft for its strength and aluminum in the air foils and other major components due to its ability to resist corrosion. Tables show the material properties for carbon steel and aluminum.

TABLE 8. MATERIAL PROPERTIES FOR CARBON STEEL

CARBON STEELS - Rephosphorized & Resulphurized

Grade	Type of Processing	Estimated Minimum Values Tensile Strength psi	Yield Strength psi	Brinell Hardness	Average Machinability Rating (Cold Drawn 1212-100%)
1006	Hot rolled	43,000	24,000	86	
	Cold drawn	48,000	41,000	95	50
1008	Hot rolled	44,000	24,500	86	
	Cold drawn	49,000	41,500	95	55
1010	Hot rolled	47,000	26,000	95	
	Cold drawn	53,000	44,000	105	55
1018	Hot rolled	58,000	32,000	116	
	Cold drawn	64,000	54,000	126	70

TABLE 9. MATERIAL PROPERTIES FOR ALUMINUM 6061-T6

Mechanical Properties			
Hardness, Brinell	95	95	AA; Typical; 500 g load; 10 mm ball
Hardness, Knoop	120	120	Converted from Brinell Hardness Value
Hardness, Rockwell A	40	40	Converted from Brinell Hardness Value
Hardness, Rockwell B	60	60	Converted from Brinell Hardness Value
Hardness, Vickers	107	107	Converted from Brinell Hardness Value
Ultimate Tensile Strength	310 MPa	45000 psi	AA; Typical
Tensile Yield Strength	276 MPa	40000 psi	AA; Typical
Elongation at Break	12 %	12 %	AA; Typical; 1/16 in. (1.6 mm) Thickness
Elongation at Break	17 %	17 %	AA; Typical; 1/2 in. (12.7 mm) Diameter
Modulus of Elasticity	68.9 GPa	10000 ksi	AA; Typical; Average of tension and compression. Compression modulus is about 2% greater than tensile modulus.

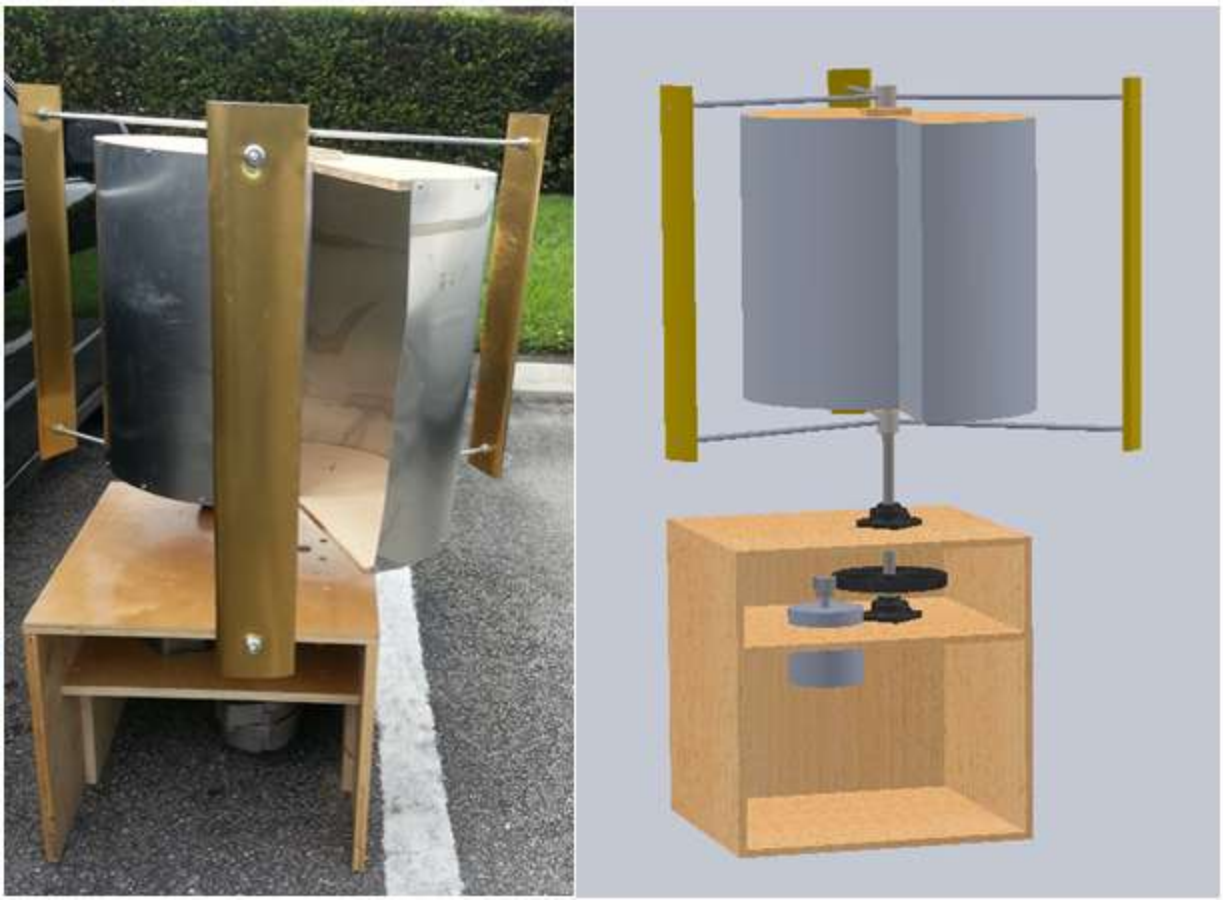

FIGURE 42. COMPLETED PROTOTYPE DESIGN

MANUFACTURING AND SIMULATIONS

Using the research and data collected, a scale solid works model was designed. Figure 48 shows the final scale model of the turbine. The prototype has a combination of Savonius and Darrieus blades. Since the Darrieus is not self-starting, Savonius blades are incorporated to get the turbine moving.

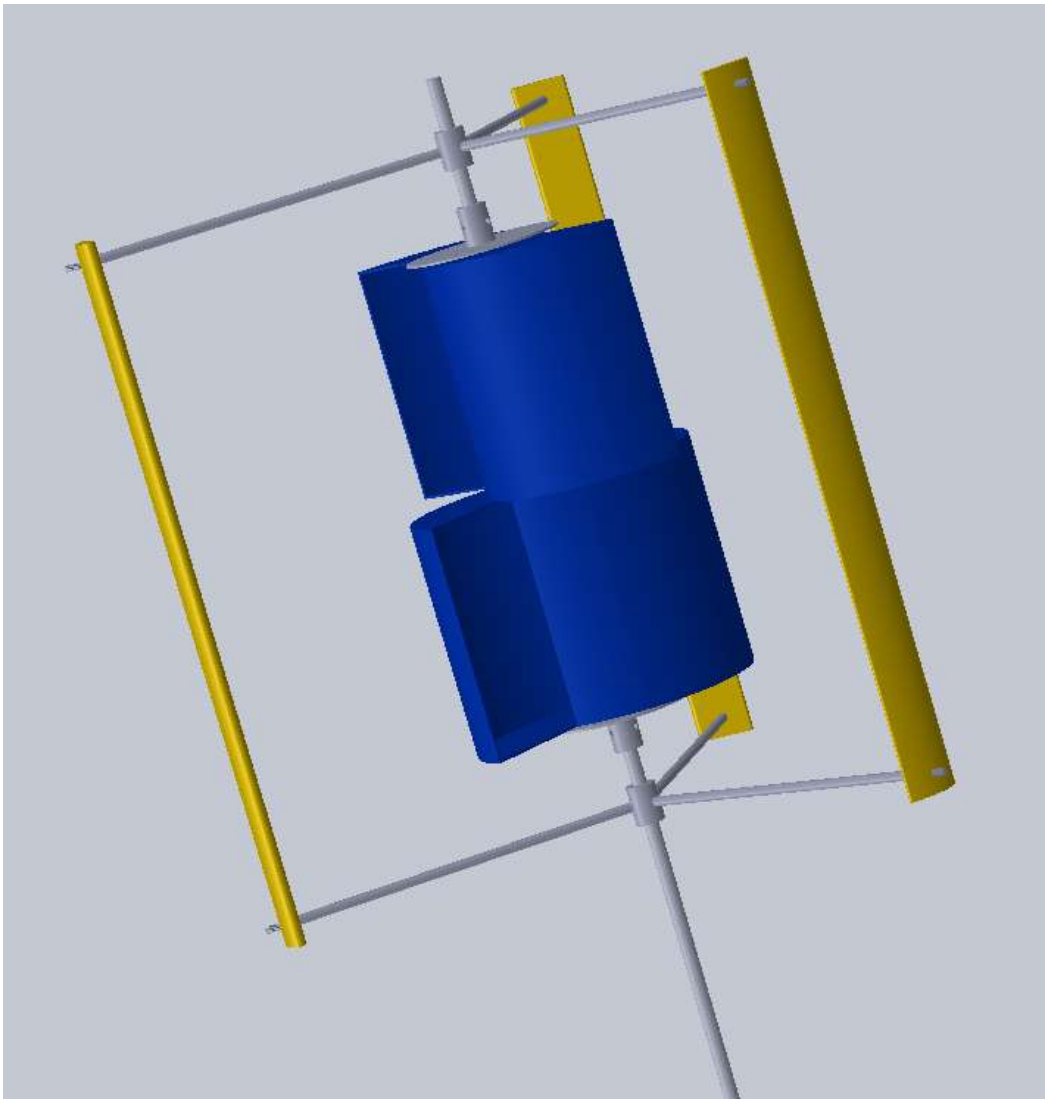

FIGURE 43. SCALE SOLIDWORKS MODEL

Figure 43 shows the 3 Darrieus blades, 4 Savonius blades, the shaft, 2 collars for the Darrieus blades and 2 collars attached to plates for the Savonius blades. At this point we realized we needed at least 2 sets of Savonius rotors stacked one over the other and oriented at 90 degrees. This designed may be used for future for optimization.

Designing efficient Darrieus turbine blades was one of the most challenging parts of the project. The blades are made of durable lightweight material. A mold is created and used to produce all 3 blades. The material selected for the blades is Aluminum 6061–T6.

The blades are filled with foam to keep them rigid and avoid distortion. Each blade is 2 feet long with an airfoil profile. The procedure for creating the Darrieus blades and Savonius Rotors is illustrated in Fig. 48-55.

FIGURE 44. ALUMINUM SHEET BEING WRAPPED AROUND THE MOLD

FIGURE 45. FORMED ALUMINUM SHEET

FIGURE 46. FOAM INSERT

FIGURE 47. ALUMINUM SHEET WRAPPED AROUND THE FOAM INSERT

FIGURE 48. COMPLETED DARRIEUS TURBINE BLADE

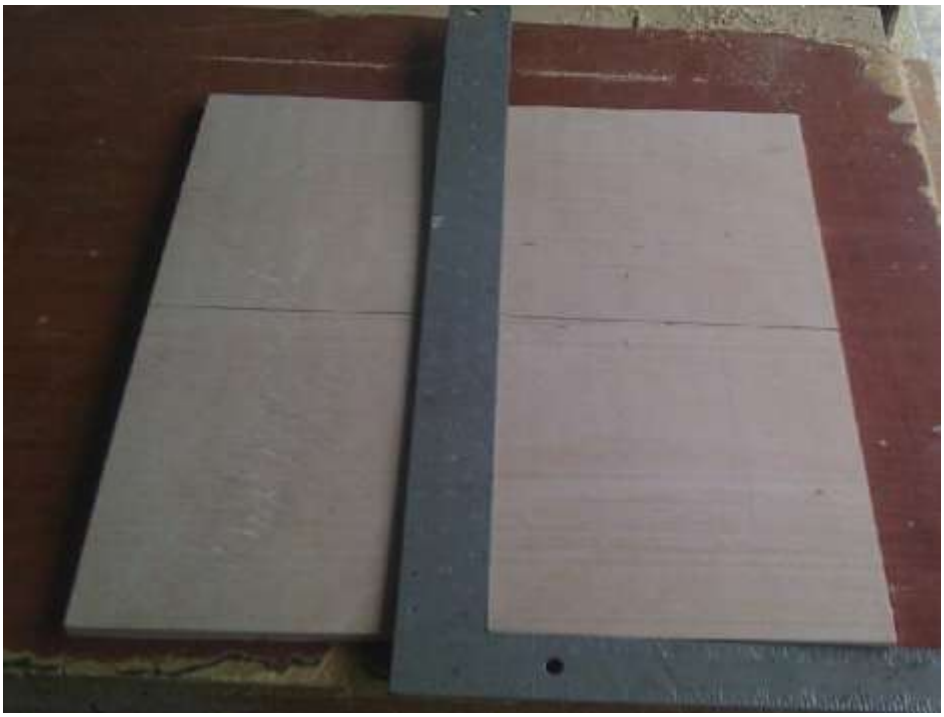

FIGURE 49. PLYWOOD FOR SAVONIUS ROTOR

FIGURE 50. DRAWING CIRCLES FOR THE SAVONIUS SCOOPS

FIGURE 51. CUT SAVONIUS ROTOR CAPS

After the prototype was built we tested the design using a fan and some of the tools in fig. 46.

FIGURE 52. TOOLS USED TO TEST MODEL

A tachometer was utilized to measure angular frequency, a multi-meter was used to measure voltage and an anemometer was used to measure wind speed. We also cross checked the wind speed using a pitot-tube. The fan was placed 7 feet away from the model, we started at a windspeed of 20 miles per hour and decreased incrementally. Experimental data on the power generated is graphed in a wind speed vs. voltage curve in figure 47.

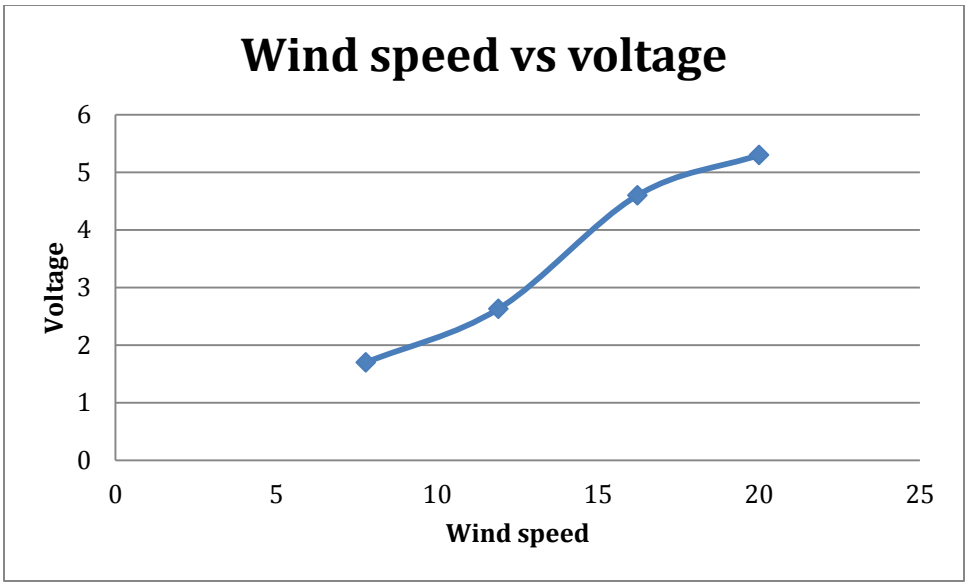

FIGURE 53. TESTED WIND SPEEDS

The results of the testing prove that we can indeed harness the power of the energy created by automobiles on the highway. At 7 miles per hour we were able to create 1.5 volts. Also, the model was tested without the use of gears, with the addition of the gears; we hope to amplify the power output by a factor of 5.

CONCLUSION

Conclusively, extensive data is collected on wind patterns produced by vehicles on both sides of the highway. Using the collected data, a wind turbine is designed to be placed on the medians of the highway. Although one turbine may not provide adequate power generation, a collective of turbines on a long strip of highway has potential to generate a large amount of energy that can be used to power streetlights, other public amenities or even generate profits by selling the power back to the grid. This design concept is meant to be sustainable and environmentally friendly. Additionally, a wind turbine powered by artificial wind has a myriad of applications. Theoretically any moving vehicle can power the turbine such as an amusement park ride or freight train. The highway wind turbine can be used to provide power in any city around the globe where there is high vehicle traffic.

REFERENCES

Highway Helical Wind Turbine Project (Next Generation Highway's Potential For. (2012, November 20). (Department of Mechanical Engineering YCET Kollam. Kerala) Retrieved February 14, 2013, from Youtube.com: http://www.youtube.com/watch?v=8g5G0LXCNDM

Global Statistics. (n.d.). Retrieved from Global Wind Energy Council: http://www.gwec.net/global-figures/wind-energy-global-status/

Joe. (2007, April 11). *Archinect*. Retrieved March 15, 2013, from Arizona State University (Joe): http://archinect.com/blog/article/21451130/here-goes-please-comment

Alternative Energy Systems and Application Mississippi State University

B.K Hodge January 2009, John Wiley & Sons Inc.

Richard G. Budynas, J. K. (2012). *Shigley's Mechanical Engineering Design.* New York: McGraw-Hill.

Abbot, I. H. (1959). *Theory of Wing Sections.* New York: Dover Publications, Inc.

Jacobs, E. N. (1939). *Airfoil Characteristis as Affected by Variations of the Reynolds Number.* National Advisory Committee for Aeronautics.

Riegels, F. W. (1961). *Airfoil Sections.* Washington Dc: Butterworth Inc.

APPENDIX A: SELECTED AIRFOIL PROFILES

NACA 0012 AIRFOILS

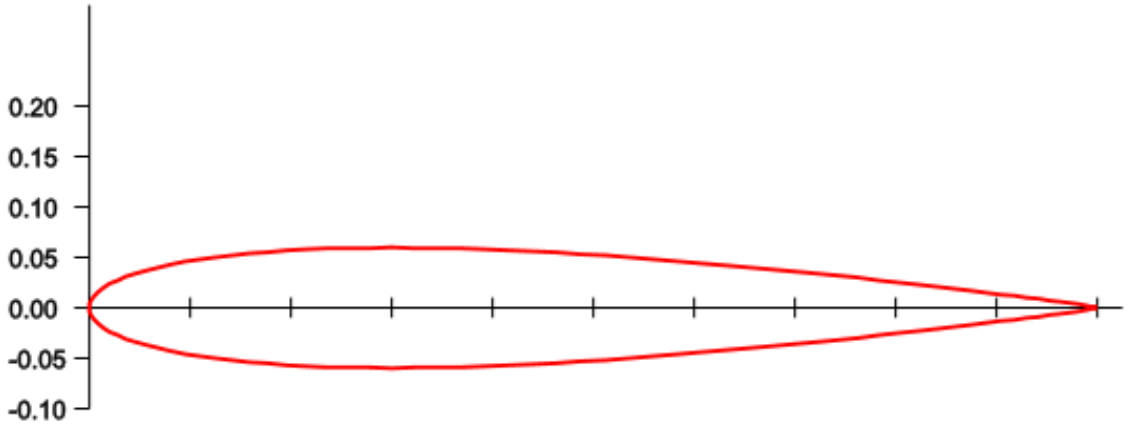

Thickness:	12.0%
Camber:	0.0%
Trailing edge angle:	58.6°
Lower flatness:	12.0%
Leading edge radius:	1.7%

Max C_L:	0.962
Max C_L angle:	15.0
Max L/D:	36.958
Max L/D angle:	7.5
Max L/D C_L:	0.842
Stall angle:	7.5
Zero-lift angle:	0.0

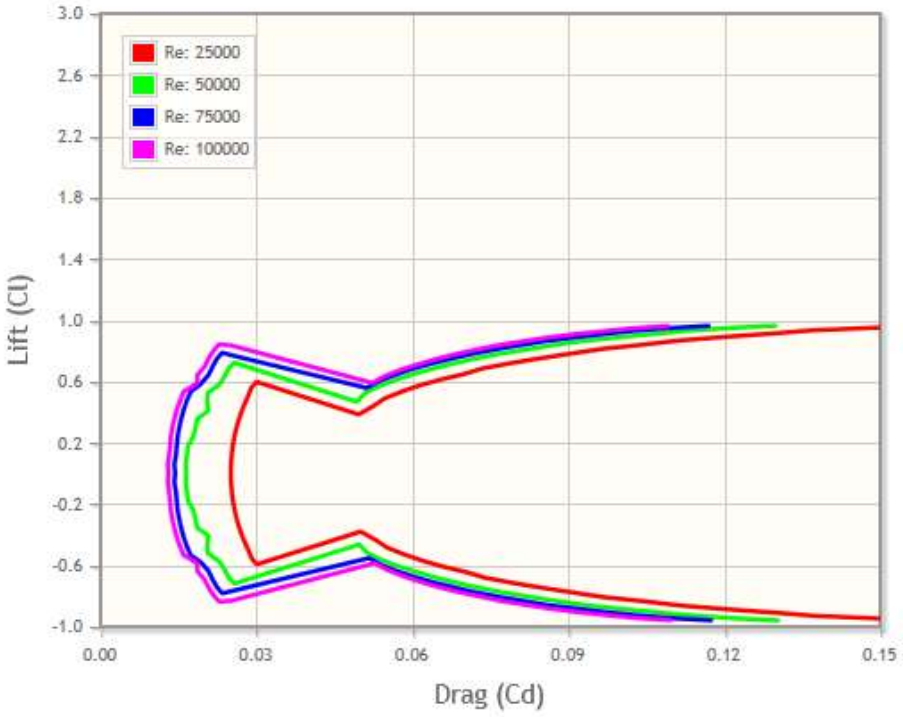
Re: 25000
Re: 50000
Re: 75000
Re: 100000
Lift (Cl)
Drag (Cd)
3.0
2.6
2.2
1.8
1.4
1.0
0.6
0.2
-0.2
-0.6
-1.0
0.00
0.03
0.06
0.09
0.12
0.15

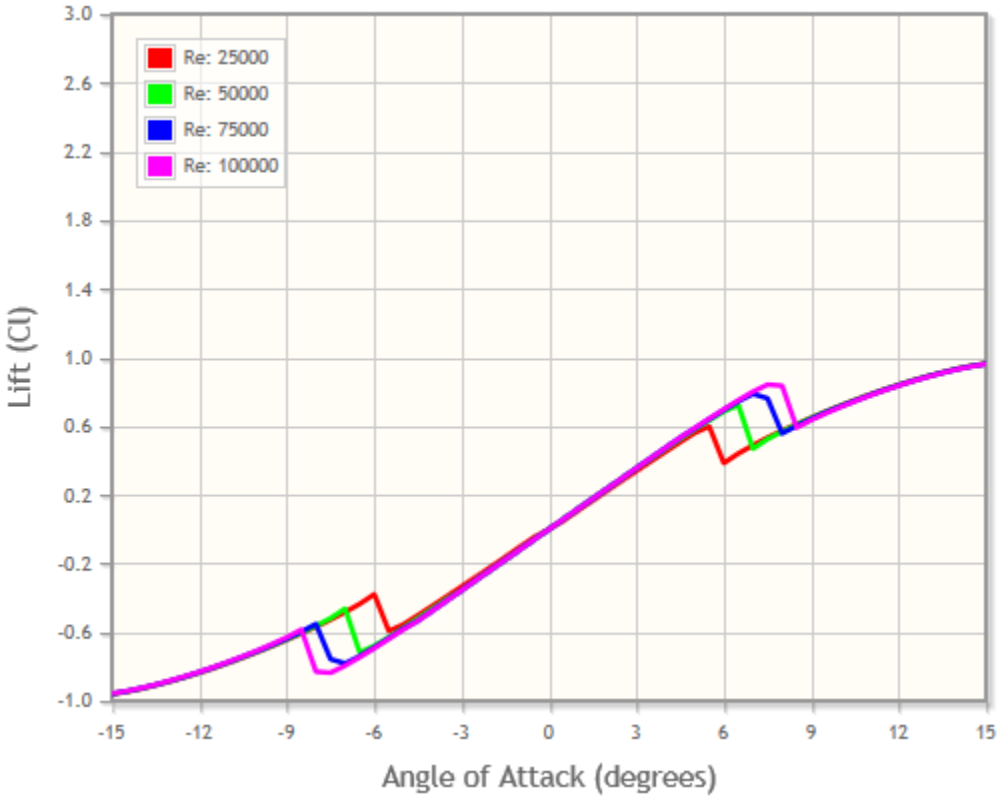
Re: 25000
Re: 50000
Re: 75000
Re: 100000
Lift (Cl)
Angle of Attack (degrees)
3.0
2.6
2.2
1.8
1.4
1.0
0.6
0.2
-0.2
-0.6
-1.0
-15
-12
-9
-6
-3
0
3
6
9
12
15

NACA 0018

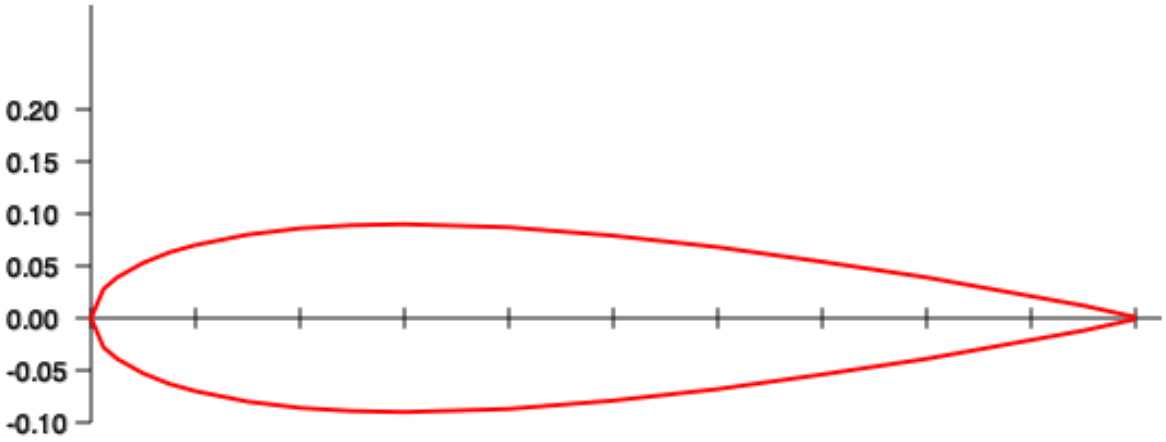

Thickness:	18.0%	**Max C_L:**	1.077
Camber:	0.1%	**Max C_L angle:**	15.0
Trailing edge angle:	24.5°	**Max L/D:**	34.864
Lower flatness:	24.2%	**Max L/D angle:**	5.5
Leading edge radius:	5.2%	**Max L/D C_L:**	0.686
		Stall angle:	11.5
		Zero-lift angle:	0.0

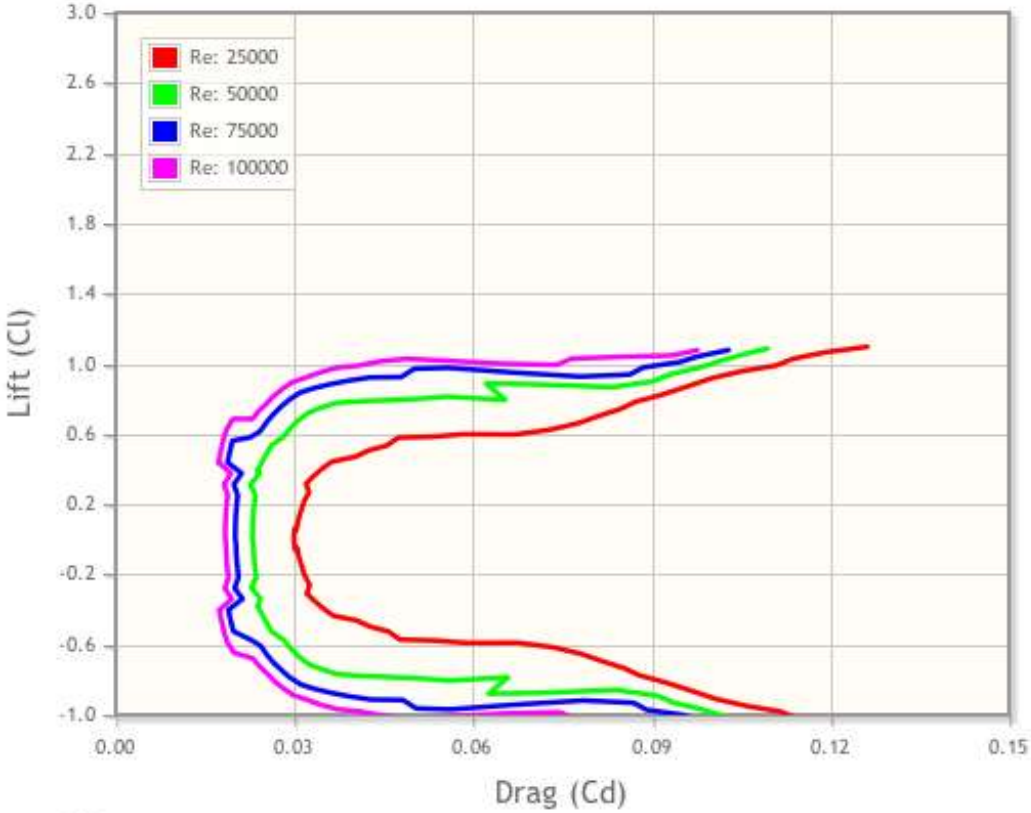
Re: 25000
Re: 50000
Re: 75000
Re: 100000
Lift (Cl)
Drag (Cd)
3.0
2.6
2.2
1.8
1.4
1.0
0.6
0.2
-0.2
-0.6
-1.0
0.00
0.03
0.06
0.09
0.12
0.15

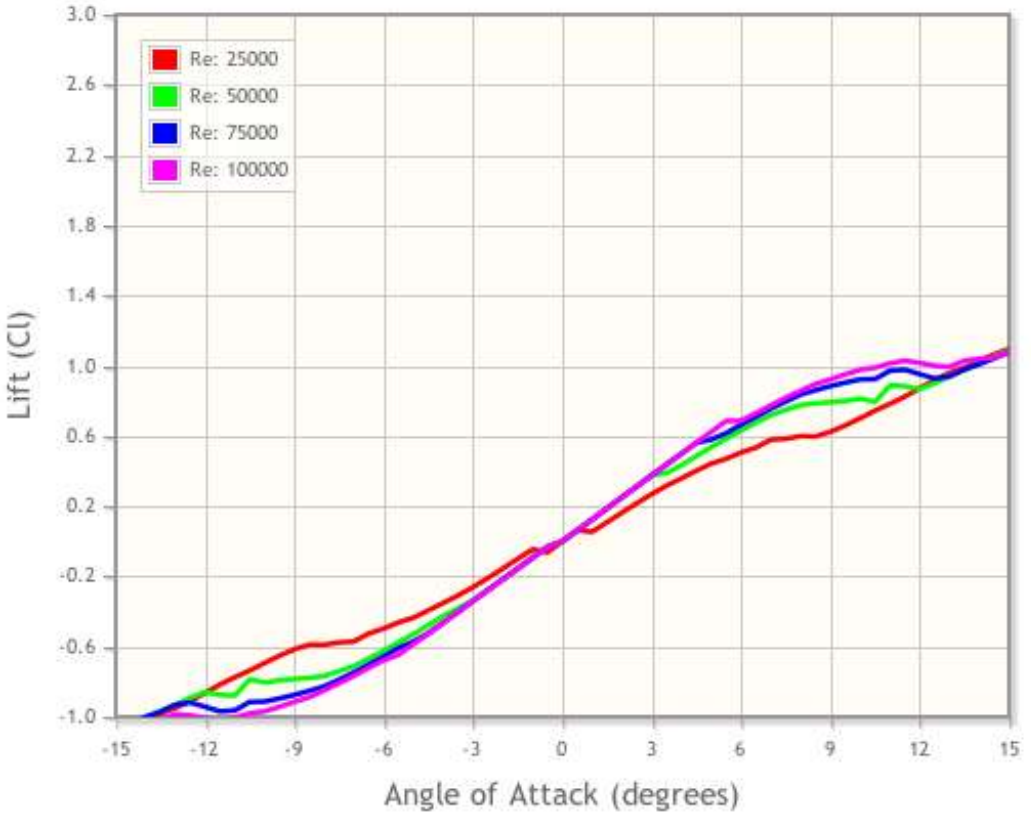
Re: 25000
Re: 50000
Re: 75000
Re: 100000
Lift (Cl)
Angle of Attack (degrees)
3.0
2.6
2.2
1.8
1.4
1.0
0.6
0.2
-0.2
-0.6
-1.0
-15
-12
-9
-6
-3
0
3
6
9
12
15

NACA 4415

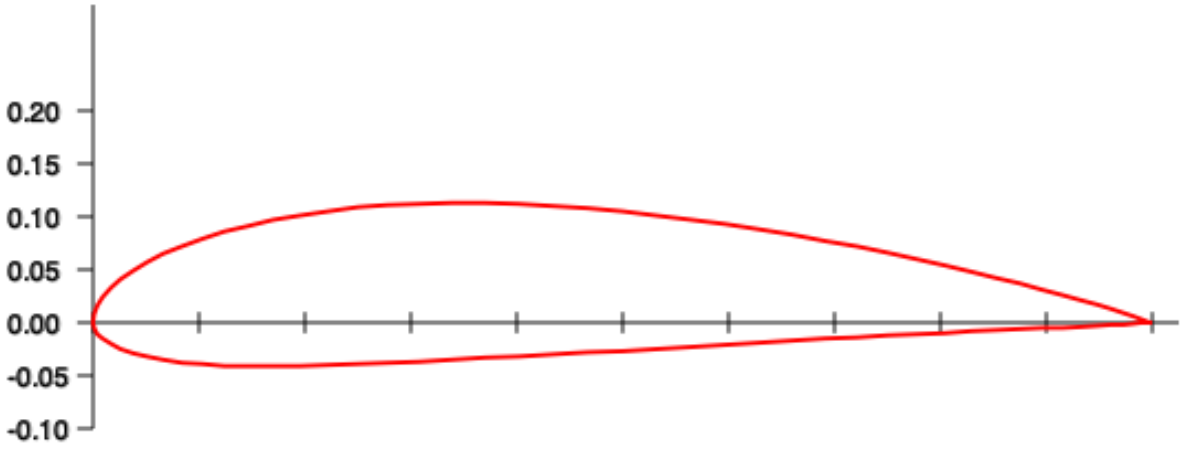

Thickness:	15.0%	**Max C_L:**	1.643
Camber:	4.0%	**Max C_L angle:**	14.0
Trailing edge angle:	25.6°	**Max L/D:**	55.43
Lower flatness:	58.9%	**Max L/D angle:**	6.0
Leading edge radius:	2.6%	**Max L/D C_L:**	1.172
		Stall angle:	14.0
		Zero-lift angle:	-4.0

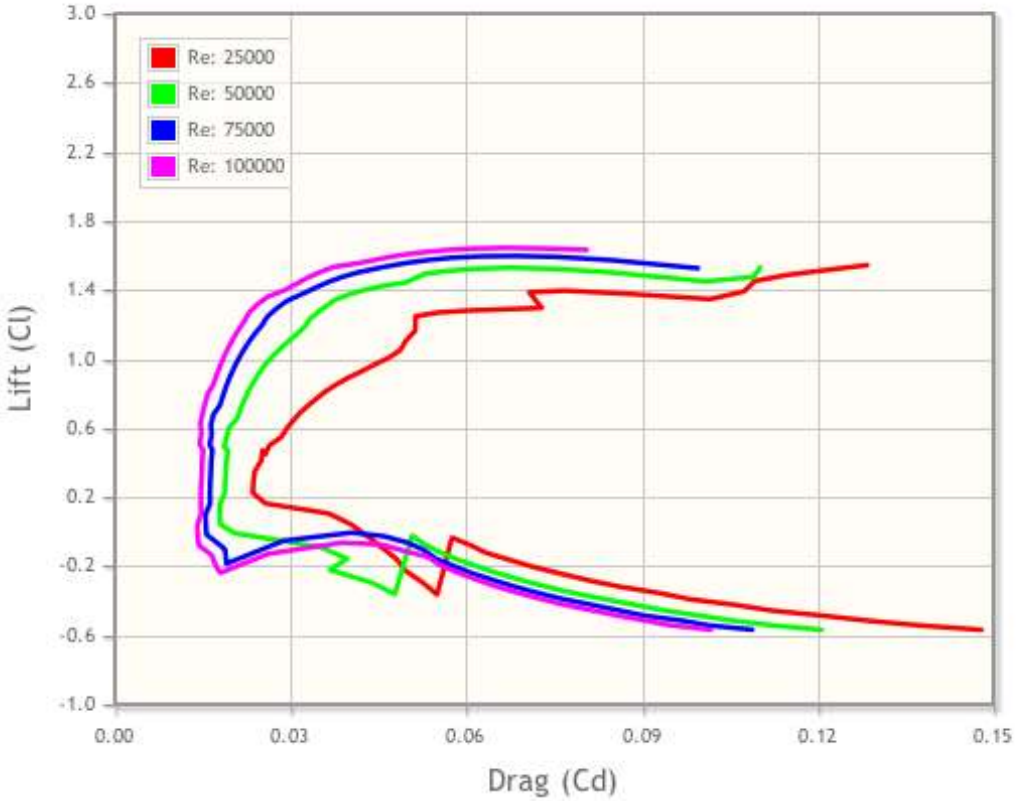
Re: 25000
Re: 50000
Re: 75000
Re: 100000
Lift (Cl)
Drag (Cd)
3.0
2.6
2.2
1.8
1.4
1.0
0.6
0.2
-0.2
-0.6
-1.0
0.00
0.03
0.06
0.09
0.12
0.15

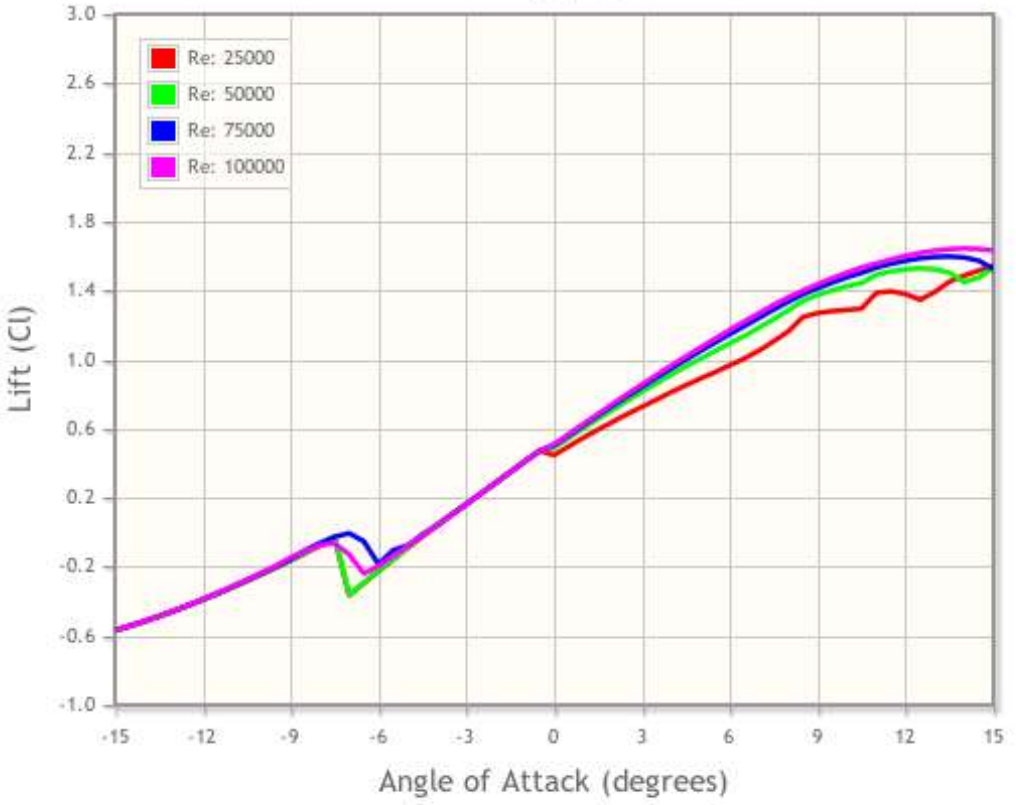
Re: 25000
Re: 50000
Re: 75000
Re: 100000
Lift (Cl)
Angle of Attack (degrees)
3.0
2.6
2.2
1.8
1.4
1.0
0.6
0.2
-0.2
-0.6
-1.0
-15
-12
-9
-6
-3
0
3
6
9
12
15

APPENDIX B: MATLAB CODE FOR SYSTEM GRAPH ANALYSIS

```
function SystemDynamics

clear all;

windspeed = 5; %miles per hour
v = windspeed*1609/3600; %windspeed in meters per second
Dt= .914;%diameter of turbine in meters
lb = .609; %length of turbine blades in meters
As= Dt*lb;
% Pw = (1/2)*density*As*v^3; Total power that can be generated by the
% turbine
Pw = .602*As*v^3; %at standard temperature and pressure STP = 293K and
101.3KPA
Cp= .40; %Turbine Efficiency
Pm= Cp*Pw; % Actual power that can be generated by the turbine
r= .457; %radius swept by the wind turbine
omega = (v/r)/(2*pi); %angular velocity of wind turbine in rev per second
Torque = Pm/omega; % Torque
tl= .101; %base length of turbine blade in meters

%Known values in system Graph
J= pi*(Dt^4-(Dt-2*tl)^4)/64 %lb*tl/12)*(lb^2+tl^2); Second moment of inertia
B1=.1; %Damper 1
B2=.1; %Damper 2
N1= 90;% Number of teeth on driven gear
N2= 18; % Number of teeth on driving gear
Ng= N1/N2; %Gear Ratio
L= 1; %Inductor in generator
R1= 8; %Resistor in generator
Nt= 20000;
R2= 6; %ohms lightbulb
Kv= 12.5; % of revs per minute motor will turn when one volt is applied
without a load
Ts= Torque; %input torque
%Matrixvalues

A= -(B1+Ng^2*B2)/J;
B= -(Ng*Kv)/L;
C= -(Kv*Ng)/J;
D= -(R2+R1)/L;


MatrixB = [A B; C D]

    t1 =0;      % starting time
    t2 = .01;   % ending time
    y0 = omega;      % initial condition
    u0 = 0;      % initial condition
    h = .0005;     % time step

    [t_rk, w_rk,z_rk] = RungeKutta( t1, t2, h, y0, u0)
```

```
    figure
    plot(t_rk,w_rk,'--b', 'linewidth', 2);
    title_handle = title('Angular Velocity vs. Time');

    xlabel('Time (s)')
    ylabel('Angular Velocity m/s')


    figure
    plot(t_rk,z_rk,'--g', 'linewidth', 2);
    title_handle = title('Current Through The Inductor Over Time');
    xlabel('Time (s)')
    ylabel('Current through Inductor (Amps)')

end

function f = func(t, y, u);
windspeed = 5; %miles per hour
v = windspeed*1609/3600; %windspeed in meters per second
Dt= .914;%diameter of turbine in meters
lb = .609; %length of turbine blades in meters
As= Dt*lb;
% Pw = (1/2)*density*As*v^3; Total power that can be generated by the
% turbine
Pw = .602*As*v^3; %at standard temperature and pressure STP = 293K and
101.3KPA
Cp= .40; %Turbine Efficiency
Pm= Cp*Pw; % Actual power that can be generated by the turbine
r= .457; %radius swept by the wind turbine
omega = (v/r)/(2*pi); %angular velocity of wind turbine in rev per second
Torque = Pm/omega; % Torque
tl= .101; %base length of turbine blade in meters

%Known values in system Graph
J= pi*(Dt^4-(Dt-2*tl)^4)/64 %lb*tl/12)*(lb^2+tl^2); Second moment of inertia
B1=.1; %Damper 1
B2=.1; %Damper 2
N1= 90;% Number of teeth on driven gear
N2= 18; % Number of teeth on driving gear
Ng= N1/N2; %Gear Ratio
L= 1; %Inductor in generator
R1= 8; %Resistor in generator
Nt= 20000;
R2= 6; %ohms lightbulb
Kv= 12.5; % of revs per minute motor will turn when one volt is applied
without a load
Ts= Torque; %input torque
%Matrixvalues

    Tss= Torque+(.7*Torque)*sin(pi*t);

    f = (1/J)*(Tss-B1*y-Ng*(u*Kv+B2*Ng*y));
end

function g = myfunc2(t, y, u);
```

```
windspeed = 5; %miles per hour
v = windspeed*1609/3600; %windspeed in meters per second
Dt= .914;%diameter of turbine in meters
lb = .609; %length of turbine blades in meters
As= Dt*lb;
% Pw = (1/2)*density*As*v^3; Total power that can be generated by the
% turbine
Pw = .602*As*v^3; %at standard temperature and pressure STP = 293K and
101.3KPA
Cp= .40; %Turbine Efficiency
Pm= Cp*Pw; % Actual power that can be generated by the turbine
r= .457; %radius swept by the wind turbine
omega = (v/r)/(2*pi); %angular velocity of wind turbine in rev per second
Torque = Pm/omega; % Torque
tl= .101; %base length of turbine blade in meters

%Known values in system Graph
J= pi*(Dt^4-(Dt-2*tl)^4)/64 %lb*tl/12)*(lb^2+tl^2); Second moment of inertia
B1=.1; %Damper 1
B2=.1; %Damper 2
N1= 90;% Number of teeth on driven gear
N2= 18; % Number of teeth on driving gear
Ng= N1/N2; %Gear Ratio
L= 1; %Inductor in generator
R1= 8; %Resistor in generator
Nt= 20000;
R2= 6; %ohms lightbulb
Kv= 12.5; % of revs per minute motor will turn when one volt is applied
without a load
Ts= Torque; %input torque
%Matrixvalues

    g = (1/L)*(-u*(R2+R1)-Kv*Ng*y);
end

function [t,w,z] = RungeKutta( t1, t2, h, y0,u0 )
    n = round((t2-t1) / h) + 1;
    w(1) = y0;
    t(1) = t1;
    z(1) = u0;

for i = 1:n-1
        t(i+1) = t1 + i*h;
        k1 = h * func(t(i), w(i), z(i));
        q1 = h * myfunc2(t(i), w(i), z(i));

        k2 = h * func(t(i) + h/2, w(i) + k1/2, z(i)+q1/2);
        q2 = h * myfunc2(t(i) + h/2, w(i) + k1/2, z(i)+q1/2);


        k3 = h * func(t(i) + h/2, w(i) + k2/2, z(i) +q2/2);
        q3 = h * myfunc2(t(i) + h/2, w(i) + k2/2, z(i) +q2/2);


        k4 = h * func(t(i+1), w(i) + k3, z(i) + q3);
```

```
        q4 = h * myfunc2(t(i+1), w(i) + k3,z(i) + q3);

    w(i+1) = w(i) + (1/6) * (k1 + 2 * (k2 + k3) + k4)
    z(i+1) = z(i) + (1/6) * (q1 + 2 * (q2 + q3) + q4)
end
end
```